

An-Najah National University

Faculty of Graduate Studies

Electrochemical properties of Sol-gel WO₃ films Co-doped with Ti and Zn

By

Madleen Ahmad Mohammad Albalshi

Supervisor

Dr. Iyad Saadeddin

Co-Supervisor

Dr. Mohammed Suleiman

**This Thesis is Submitted in Partial Fulfillment of the Requirements for
the Degree of Master of Physics, Faculty of Graduate Studies, An-
Najah National University - Nablus, Palestine.**

2016

Electrochemical properties of Sol-gel WO₃ films Co-doped with Ti and Zn

By

Madleen Ahmad Mohammad Albalshi

This thesis was defended successfully on 12 / 1/2016, and approved by:

Defense Committee Members

Signature

– **Dr. Iyad Saadeddin / Supervisor**


.....

– **Dr. Mohammed Suleiman / Co-Supervisor**


.....

– **Dr. Rabab Jarrar / External Examiner**


.....

– **Prof. Ismail Warad / Internal Examiner**


.....

III

Dedication

To my Parents

To my husband "Jafar"

To my son Iyas

To my future daughter

Acknowledgment

After the Almighty Allah, I would like to express my sincere thanks and heartfelt gratitude to my supervisor Dr. Iyad Saadeddin for his guidance, helpful efforts, excellent advices, and encouragement, and to my Co-supervisor Dr. Mohammed Suleiman.

Special thanks to the members working in the physics and chemistry departments laboratories for their help and support, especially, Mr. Mohammad Bahjat, and Mr. Nafeth Zakrea.

I would also like to take this opportunity to express my deep thankfulness to my family (my father, my mother, my sisters and their husbands, my brothers and their wives) and my husband's family for the continuous support and encouragement.

Finally, I strongly express my profound gratitude to my dearly husband Jafar and my son Iyas for the moral support and patience during my study.

أنا الموقعة أدناه مقدمة الرسالة التي تحمل العنوان:

Electrochemical properties of Sol-gel WO_3 films Co-doped with Ti and Zn

أقر بان ما اشتملت عليه هذه الرسالة إنما هو نتاج جهدي الخاص، باستثناء ما تمت الإشارة إليه حيثما ورد، وان هذه الرسالة ككل من أو جزء منها لم يقدم من قبل لنيل أية درجة أو بحث علمي أو بحثي لدى أية مؤسسة تعليمية أو بحثية أخرى.


Declaration

The work provided in this thesis, unless otherwise referenced, is the researcher's own work, and has not been submitted elsewhere for any other degree or qualification.

Student's Name:

اسم الطالبة: مدينا أحمد محمد البلمست

Signature:

التوقيع: 

Date:

التاريخ: ٢٠١٦ / ١١ / ١٣

Table of Contents

No.	Content	Page
	Dedication	III
	Acknowledgement	IV
	Declaration	V
	Table of Contents	VI
	List of Tables	VIII
	List of Figures	IX
	Abstract	XI
	Chapter One: Introduction	1
1.1	Objectives	2
1.2	Why WO ₃ based thin films?	2
1.3	Hypothesis	3
1.4	Previous Studies	3
	Chapter Two: Fundamentals and theoretical background	7
2.1	Chromism	8
2.2	Electrochromism	9
2.2.1	Design and operation of electrochromic devices (ECDs)	9
2.2.2	Applications of electrochromic devices	11
2.2.3	Types of electrochromic devices	13
2.3	Background on tungsten and Tungsten oxide	14
2.3.1	Tungsten	14
2.3.2	Tungsten oxide (WO ₃)	15
2.4	Coloration mechanism of Tungsten oxide-based thin films	17
2.5	Electrochromic properties	18
2.5.1	Cyclic voltammetry (CV)	18
2.5.2	Chronoamperometry (CA)	20
2.6	Optical properties	22
2.7	Deposition technique of WO ₃ -based thin films	23
2.7.1	Physical Techniques	23
2.7.2	Chemical Techniques	27
	Chapter Three: Experimental Work	33
3.1	Materials and film preparation	34
3.1.1	Chemicals and Solvents	34
3.1.2	Preparation of WO ₃ based films	34
3.2	Measurements	39
3.2.1	Cyclic voltammetry (CV)	39
3.2.2	Chronoamperometry (CA)	40

VII

No.	Content	Page
3.2.3	Transmittance	41
	Chapter Four: Results and Discussion	42
4.1	Tungsten oxide doped with Titanium ($WO_3:Ti$) thin films	43
4.1.1	Cyclic Voltammetry (CV)	43
4.1.2	Chronoamperometry (CA)	43
4.1.3	Optical properties	54
4.1.4	Conclusions	55
4.2	Tungsten oxide co-doped with Ti and Zn ($WO_3: Ti:Zn$) thin films	55
4.2.1	Cyclic Voltammetry (CV)	56
4.2.2	Chronoamperometry (CA)	61
4.2.3	Optical properties	62
4.2.4	Conclusions	64
4.3	General Conclusions	64
	Suggestions for Further Works	65
	References	67
	المخلص	ب

List of Tables

No.	Table Captions	Page
Table (3.1)	List of intended structure, Tungsten (VI) chloride mass, and Titanium (II) Chloride mass used in the sol-gel preparation	36
Table (3.2)	list of intended structure, Titanium (II) Chloride mass, and Zinc (II) chloride mass used in the sol-gel preparation. All sol-gel solutions contain 1.658 gm of Tungsten (VI) chloride	37
Table (4.1)	Calculation of diffusion coefficient using Randles-Sevcik equation	48
Table (4.2)	The electrochromic properties for WO_3 doped with different molar concentration of Ti	51
Table (4.3)	The electrochromic properties for $\text{W}_{0.95}\text{Ti}_{0.05-y}\text{Zn}_y\text{O}_3$ ($\text{WO}_3\text{:Ti:Zn}$) with y values a) 0, b) 0.01, c) 0.02, d) 0.03, e) 0.04, f) 0.05	59

List of Figures

No.	Figure Captions	Page
Fig. (2.1)	Schematic diagram of the electrochromic device	10
Fig. (2.2)	Variety applications for electrochromic devices	12
Fig. (2.3)	ECWs with illustration of visible light and solar heat energy during operation.	13
Fig. (2.4)	Three different types of electrochromic devices (ECDs): (a) solution type, (b) hybrid type, and (c) battery-like type.	14
Fig. (2.5)	monoclinic structure of Tungsten oxide (WO_3) at room temperature	17
Fig. (2.6)	The reduction of W^{+6} in WO_3 to a W^{+5} state and the oxidation of M^+ to form M_2O	18
Fig. (2.7)	Voltage swept during CV experiments.	19
Fig. (2.8)	A typical cyclic voltammograms recorded for a reversible single electrode transfer reaction a) at one scan rate b) at different scan rate	20
Fig. (2.9)	Chronoamperometry curve showing current (—) response with applied potential (- -):-	21
Fig. (2.10)	Basic elements of sputtering system	24
Fig. (2.11)	A schematic shows of the electron beam evaporation process	25
Fig. (2.12)	A typical composition of a PLD technique chamber	26
Fig. (2.13)	Schematic show of sol-gel process to synthesize nanomaterials, thin films, and ceramics.	30
Fig. (2.14)	A spin coating process	31
Fig. (2.15)	Schematic presentation of the stages of the dip coating process	32
Fig. (3.1)	Steps of preparing sol-gel solution: (a) waighting, (b) stirring, (c) sonicating, (d) the color change of the solution from yellow to blue.	37
Fig. (3.2)	Procedure of WO_3 -based films deposition by dip coating process	38
Fig. (3.3)	A Potentiostat device with three electrodes electrochemical cell	40
Fig. (4.1)	Cyclic voltammetry measurements of the undoped and 5, 10, 15, 20, 25, and 30 at. % Ti doped WO_3 films at the scan rate of 100 mV/s	44
Fig. (4.2)	Dependence of (a) peak current density (J_{pa} and J_{pc}), and (b) anodic peak potential (E_{pa}) on the Ti	45

	concentration	
Fig. (4.3)	Current density with time for $\text{WO}_3:\text{Ti}$ with different Ti molar concentrations: a) WO_3 , b) $\text{W}_{0.95}\text{Ti}_{0.05}\text{O}_3$, c) $\text{W}_{0.90}\text{Ti}_{0.10}\text{O}_3$, d) $\text{W}_{0.85}\text{Ti}_{0.15}\text{O}_3$, e) $\text{W}_{0.80}\text{Ti}_{0.20}\text{O}_3$, f) $\text{W}_{0.75}\text{Ti}_{0.25}\text{O}_3$, g) $\text{W}_{0.70}\text{Ti}_{0.30}\text{O}_3$	46
Fig. (4.4)	Cyclic voltammetry measurements for (a) WO_3 film (b) $\text{W}_{0.95}\text{Ti}_{0.05}\text{O}_3$ film at different scan rates. The inset shows the reliance of J_{pa} against square root of the scan rate.	49
Fig. (4.5)	Cyclic Voltammetry of the $\text{W}_{0.95}\text{Ti}_{0.05}\text{O}_3$ film for 2 nd , 1000 th , 5000 th , and 6000 th cycles at a scan rate of 200 mV/s. The inset shows stability of the anodic charge with cycle number	52
Fig. (4.6)	$\text{W}_{0.95}\text{Ti}_{0.05}\text{O}_3$ film degradation after 6000 th cycles	53
Fig. (4.7)	Chronoamperometry of the undoped and 5, 10, 15, 20, 25, and 30 at. % Ti doped WO_3 films at potential step ± 0.5 V for 10 s	53
Fig. (4.8)	transmittance spectra for $\text{W}_{0.95}\text{Ti}_{0.05}\text{O}_3$ during CA measurements at wavelength of 633nm	55
Fig. (4.9)	Cyclic voltammetry measurements of the $\text{W}_{0.95}\text{Ti}_{0.05-y}\text{Zn}_y\text{O}_3$ with y values 0, 1, 2, 3, 4 and 5 at. % Zn at the scan rate of 100 mV/s	57
Fig. (4.10)	Dependence of (a) peak current density (J_{pa} and J_{pc}), and (b) anodic peak potential (E_{pa}) on the Ti concentration	57
Fig. (4.11)	Current density with time for $\text{W}_{0.95}\text{Ti}_{0.05-y}\text{Zn}_y\text{O}_3$ ($\text{WO}_3:\text{Ti}:\text{Zn}$) with y values a) 0, b) 0.01, c) 0.02, d) 0.03, e) 0.04, f) 0.05.	58
Fig. (4.12)	Cyclic voltammetry measurements for $\text{W}_{0.95}\text{Ti}_{0.02}\text{Zn}_{0.03}\text{O}_3$ film at different scan rates. The inset shows the reliance of J_{pa} against square root of the scan rate.	60
Fig. (4.13)	Cyclic Voltammetry of the $\text{W}_{0.95}\text{Ti}_{0.02}\text{Zn}_{0.03}\text{O}_3$ film for 2 nd , 1000 th , 5000 th , and 10000 th cycles at a scan rate of 200 mV/s. The inset shows stability of the anodic charge with cycle number	61
Fig. (4.14)	$\text{W}_{0.95}\text{Ti}_{0.02}\text{Zn}_{0.03}\text{O}_3$ film after 10000 th cycles	61
Fig. (4.15)	Chronoamperometry of the undoped and 1, 2, 3, 4, and 5 at. % Zn doped $\text{W}_{0.95}\text{Ti}_{0.05}\text{O}_3$ films at potential step ± 0.5 V for 10 s	62
Fig. (4.16)	transmittance spectra for $\text{W}_{0.95}\text{Ti}_{0.02}\text{Zn}_{0.03}\text{O}_3$ during CA measurements at wavelength of 633nm	64

Electrochemical properties of Sol-gel WO₃ films Co-doped with Ti and Zn**By****Madleen Ahmad Mohammad Albalshi****Supervisor****Dr. Iyad Saadeddin****Co-Supervisor****Dr. Mohammed Suleiman****Abstract**

WO₃ nanoparticles doped with Ti (W_{1-x}Ti_xO₃) and co-doped with Ti and Zn (W_{1-x}Ti_{x-y}Zn_yO₃) have been prepared on FTO/glass substrate, using wet chemical method (dipping in a sol-gel). The Ti molar concentration into W_{1-x}Ti_xO₃ ranges 0-30 % in steps of 5%. Best electrochromic properties were observed for composition that has Ti nominal concentration of 5% (W_{0.95}Ti_{0.05}O₃). This was evidenced from cyclic voltammetry (CV), chronoamperometry (CA), and transparency during CA measurements. The composition that gives best electrochromic properties (W_{0.95}Ti_{0.05}O₃) was chosen to prepare WO₃ nanocrystallite films co-doped with Zn for the first time (W_{0.95}Ti_{0.05-y}Zn_yO₃). The Zn molar concentration in these films varied 1-5%. From CV and CA measurements, Co-doped WO₃ films showed better electrochromic performance than Ti single doped films. From co-doped films, the best electrochromic properties were observed for films that contains 3% of Zn (W_{0.95}Ti_{0.02}Zn_{0.03}O₃). The transparency spectrum of W_{0.95}Ti_{0.02}Zn_{0.03}O₃ electrode shows a high improvement in coloration efficiency compared to the coloration efficiency of W_{0.95}Ti_{0.05}O₃ electrode. The stability of the prepared materials is also tested in H₂SO₄ electrolyte, though cycling electrodes for at least 6000 cycles.

Chapter One

Introduction

Chapter One

Introduction

1.1 Objectives

The aim of this thesis is to improve the electrochromic properties of WO_3 based thin films by doping WO_3 with Ti and/or Zn species. These thin films were grown on fluorine doped tin oxide (FTO) layer coated onto glass substrate using sol-gel method.

To find the optimum concentration of Ti species onto WO_3 thin films different atomic percentage of Ti (5-30% in steps of 5%) will be employed. Then these films with different concentration of Ti will be studied and analyzed by Cyclic Voltammetry, Chronoamperometry, and Optical experiments. After that, WO_3 thin film with optimal concentration of Ti was used to apply co-doping of Ti and Zn. The effect of co-doping on the electrochromic properties for the desired films was investigated and analyzed for the first time.

1.2 Why WO_3 based thin films?

Tungsten oxide is one of the gleaming substances in electrochromism it has been rigorously studies for its interesting electrical properties, fast response time, high coloration efficiency, reasonable stability and relatively low cost [1-3]. Physical and chemical properties make it promising material for a wide range of scientific application such as: optical switching devices, solar energy converters, smart windows, catalysis, electrocatalyst in fuel cells, and metal powder fabrications [4-9].

1.3 Hypothesis

Tungsten oxide thin film has a wide range of technological applications in various fields. Doping these films, with other substances, is known to modify their structure and hence affect their crystal structure and properties [2]. Therefore, WO_3 thin film will be adjusted in their structure and characteristics by co-doping them with appropriate concentration of Ti and Zn substances. In addition influence on electrochromic properties will be illustrated by observing and analyzing this new substance from WO_3 thin film.

1.4 Previous Studies

The electrochromic performance of Tungsten oxide is highly characterized thus; it attracts researcher's attention to know more about this brilliant material [2]. It is first reported by Deb [10], and then further studies published on these popular electrochromic films.

Hyun and Kyung study the effect of Tungsten oxide nanopowders size on their electrical properties. They found that the particle size of the powder is strongly related to the electrical properties of WO_3 thin films. Thus they suggested nano crystalline Tungsten oxide thick film to be used for gas sensors applications [11].

Bertus *et al* prepare smooth and homogenous Tungsten oxide thin films using the chemical method spray pyrolysis and found that this method could enhance the coloration efficiency transition modulation and cyclic stability of Tungsten oxide thin films [12]. On the other hand Hepel and Tewksbury reported that the electrodeposition technique could enhance

Tungsten oxide properties in a way that is cannot be achieved by any other techniques [13].

Recent study improve the coloration efficiency of Tungsten oxide films using magnetron sputtering method to reach maximum coloration efficiency of $79 \text{ cm}^2/\text{c}$ which is the first time observed for the film deposited at DC power of 150 w and pulsing frequency of 25 kHz [14].

Other researchers prefer to use sol-gel technique in Tungsten oxide thin films preparation processes, this returns to their interesting properties since it is cheap, low temperature technique, and used in several fields as in optics, energy, electronics, space, and medicine [15]. As an example, Badilescu and ashirt used this method to study the characterization of Tungsten oxide films by comparing the optical and electrochromic properties of different films of Tungsten oxide prepared either by thermal treatment or by solvent extraction [16]. On the other hand, Catalini and his group used sol-gel method to prepare Tungsten oxide films at different temperature and then analyze the characterization of the prepared films using scanning electron microscope and X-ray diffraction [17].

To improve the efficiency of Tungsten oxide films as an electrochromic device, researchers doped Tungsten oxide with different dopant atoms. Ahn and his group investigate the effect of SnO_2 addition to Tungsten oxide on the structural, electrochemical, and electrochromic properties of Tungsten oxide, they found that the doped films have faster response time, improved memory effect, and greater coloration efficiency by 14% than Tungsten oxide alone [18]. Other scientists use Ti atoms as the dopant elements. This

comes from its fantastic properties that make this material very resistant to the usual kinds of metal fatigue. It also has a relatively high melting point which makes it useful as a refractory metal [19].

Reich and Tsabba doped Tungsten oxide with Na atoms and then studied the change of the film's conductivity with temperature; they found that it exhibits a sharp diamagnetic step in magnetization at 91 K [20]. While, Chang and his group chose Zn atoms to be the dopant atoms, they prepared Tungsten oxide with different concentrations of Zn and different annealing temperatures. They found that Zn addition to Tungsten oxide enhanced its photoelectric properties and that the photocurrent under visible light displayed the highest value for 2% Zn-WO₃ films annealed at 400 °C [21].

Ozer and Dogan analyzed the optical properties of Ti-doped WO₃ (WO₃:Ti) films in bleached and colored states. They reported that the material color of Ti: WO₃ films has significant advantages over WO₃-based windows [22]. However, Bathe and Patil studied the effect of Ti doping on the electrochromic properties of Tungsten oxide. They concluded that at higher Ti concentrations (10 at. %) the cycle stability, charge storage capacity, and reversibility of the films are improved [23].

Various new studies choose a suitable percentage of Ti atoms and then analyze the effect of different doping percentages on several properties of Tungsten oxide. Rammana and his groups use 20% Ti as the doping percentage and then calculate the optical constants change with gradual change of temperature [24]. Furthermore, Wang and Hu prepared TiO₂ (10% at.)

doped Tungsten oxide films and investigate the effect of annealing temperature and water contents on the electrochromic properties of the prepared films using cyclic voltammograms experiments [25]

The effect of co-doping on different properties of the electrochromic based films is also studied and analyzed. Recently, Yang and his groups developed new WO_3 -based material for smart window application and found that co-doping of WO_3 with Li and other atoms in the form of $(\text{Li}_{0.083}\text{A}_{0.083}\text{WO}_3, \text{A} = \text{Na, K, Rb, and Cs})$ is more stable than mono-doping with alkali metals alone $(\text{A}_{0.083}\text{WO}_3, \text{A} = \text{Li, Na, K, Rb, and Cs})$ [26]. In addition to that, Long and Run studied the electronic properties and photocatalytic activity of nitrogen (N) and/or tungsten (W)-doped titania, they found that N and W-doped titania exhibit higher visible light photocatalytic efficiency than N- or W-doped alone [27]. Furthermore, co-doping NiO with Ti and Zn species was observed to give more enhanced properties than doping NiO with Ti alone, this is refer to better adhesion of co-doped NiO on the FTO substrate [28]. These studies are considered as indicators that co-doping with suitable species on the based films mostly have more enhanced and developed properties than mono-doping.

Chapter Two

Fundamentals and theoretical background

Chapter Two

Fundamentals and theoretical background

2.1 Chromism

Chromism is reversible change in substances' color resulting from a process caused by some form of external stimulus [29]. The type of used stimuli determines the kind of chromism. There are several kinds of chromism, which are detailed below.

- ❖ **Thermochromism** is defined as the reversible change of substances color caused by temperature change [30].
- ❖ **Photochromism** is the substances with reversible color change which result from photoirradiation [31].
- ❖ **Halochromism** is defined as the reversible color change caused by variance in PH, due to either acids or bases [32].
- ❖ **Piezochromism** is the reversible color change caused by mechanical grinding. This induced color change back to the original color when the material is dissolved or kept in dark organic solvent. A chemical that offer this event is diphenylflavylene.
- ❖ **Tribochromism** defined as the phenomenon when crystals color change during mechanical grinding (as in the case of Piezochromism), but the induced color change doesn't back to the original color if put in the dark or dissolved in an organic solvent [31].
- ❖ **Solvatochromism** is the reversible color change caused by the change of the polarity of solvent.

- ❖ **Halosolvatochromism** it is the reversible change in color upon increasing ionic strength of the medium without a chemical change of the chromophore [31].
- ❖ **Ionochromism** is the phenomenon of color change associated with the addition of ions [33].
- ❖ **Electrochromism** is defined as the process of reversible change in substances optical properties upon applied voltage. It is an old phenomenon which was discovered 44 years ago and potentially the most commercially useful form of chromism [34].

2.2 Electrochromism

2.2.1 Design and operation of electrochromic devices (ECDs)

An electrochromic (EC) material can modulate their optical properties upon the application of a voltage [35]. Due to Tungsten oxide superior optical and electrical properties, it is the preferred material for electrochromic device. The standard electrochromic device behaves as a thin film batteries which is composed of five layers backed by one substrate or positioned between two substrates by use of lamination (Fig. 2.1).

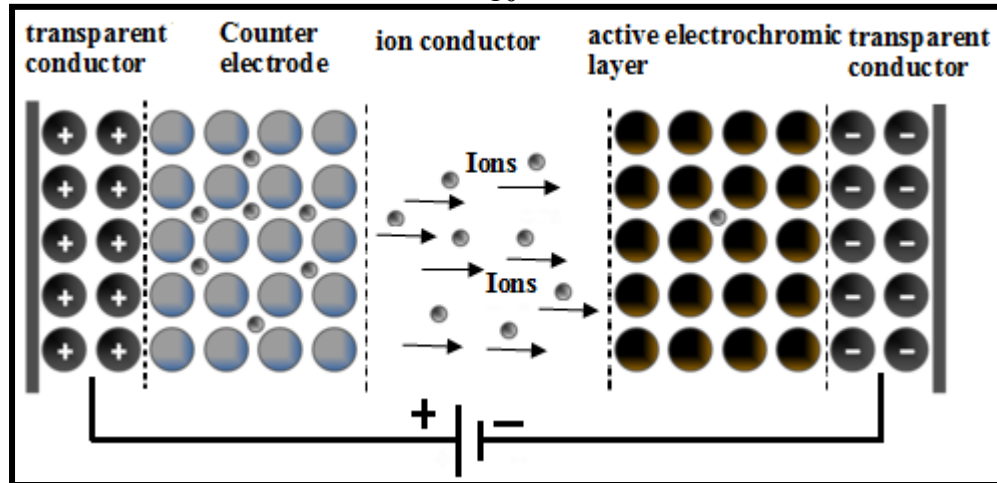


Fig. (2. 1): Schematic diagram of the electrochromic device.

The substrates are normally of glass, but plastic works too. The central part is called electrolyte (ion conductor), which conducts ion but not electrons. This can be organic material or inorganic, solids or liquids. The ions must have small size to move easily in an electric field such as proton (H^+) and lithium ions (Li^+). In early devices and for cyclic voltammetry measurements, the used electrolytes are liquids or semi-solid (e.g. H_2SO_4 solution for proton conduction and propylene carbonate with $LiClO_4$ for Li^+ conduction). The electrolyte have to be transparent, neutral coloring, and shouldn't react with the two insertion electrochromic electrodes, in which it is sandwiched between, during deposition and cycling. Proton conductors are commonly associated with higher ionic conductivity while lithium-based electrolytes show higher stability. This electrolyte bounds on an active electrochromic film (WO_3 is a perfect example) eligible of conducting electrons as well as ions. On the opposite side of the electrolyte there is an electrochromic film which stores ions (Counter electrode) and has electrochromic properties complementary to those on the first

electrochromic film. This central three layer structure is located between electrically conducting transparent films. For this purpose, transparent conductive oxide (TCO deposited onto glass or plastic) is used [36-38]. N-type TCO thin films are generally based on In_2O_3 : Sn (ITO) and SnO_2 : F (FTO) using commonly deposition techniques of PVD and CVD respectively, FTO has the advantage of being less costly than ITO and readily available on large area glass panes [28].

When a few volts are applied between the transparent electrical conductors, ions are traveled regularly between the electrochromic film and the ion storage film. The electrons move from the transparent conductors which result in a modification in the optical properties. A converted voltage, return the original properties. The electrochromic device coloration able to be modified at any intermediate scale, thus the device shows open-circuit memory as a battery.

2.2.2 Applications of electrochromic devices

There are many uses of substances which modify their optical properties reversibly via applying a little voltage signal. Fig. (2.2) show some applications of electrochromic devices like: EC windows, EC mirrors, EC displays, smart sunroofs, filters, and smart glass wears [28, 39].

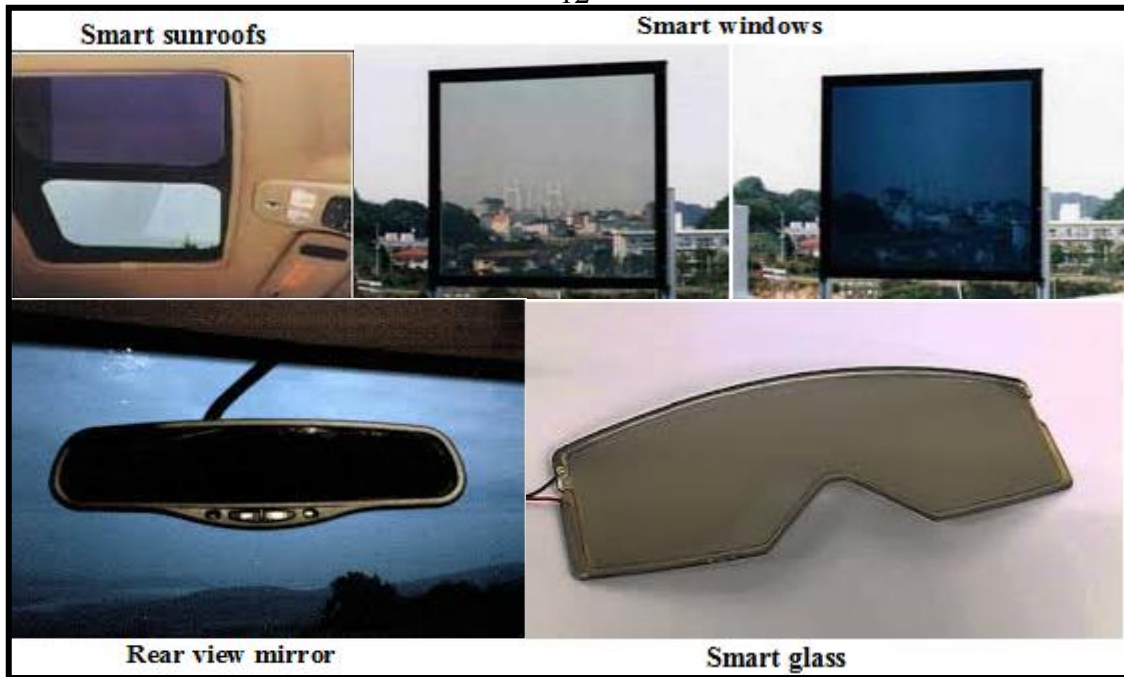


Fig. (2.2): Variety applications for electrochromic devices.

EC windows or smart windows can automatically control the amount of light and solar energy passing through the windows, by modulating their optical properties depending on the weather. Thus its benefits exceeds its importance as a transparent surface to an efficient element in energy saving; it can provide human with excellent climate that make them always relax. When EC window is in its bleached states, the visible light and part of solar heat penetrate the EC window to indoor. The transmitted visible light from electromagnetic radiation and solar heat energy can be minimized when the EC windows in its colored state (Fig. 2.3). The first commercial device of EC window was in stadtparkass bank in Dresden, Germany [40].

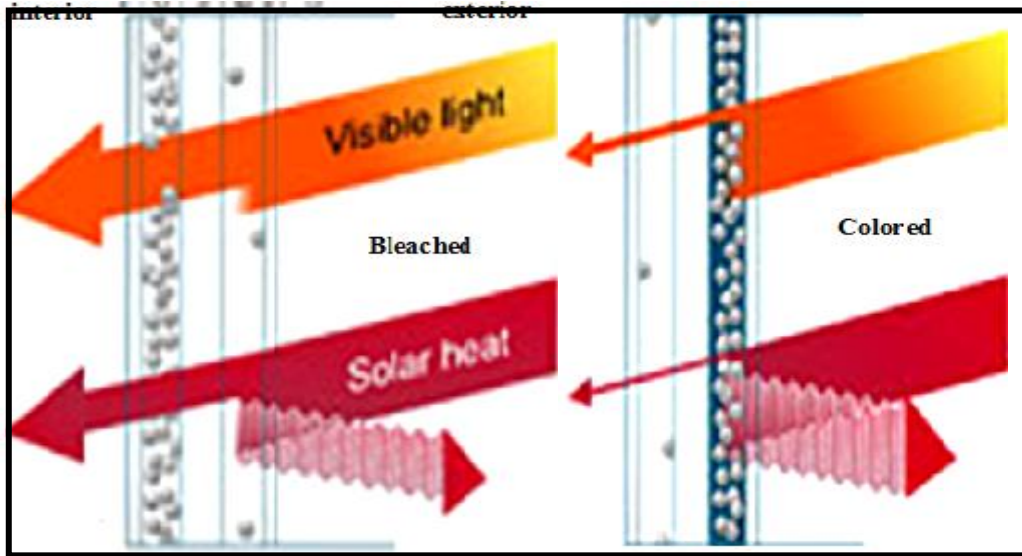


Fig. (2.3): ECWs with illustration of visible light and solar heat energy during operation.

Antithesis to smart windows, EC mirrors are already wide-spread commercially available. The construction of EC mirrors is the same as smart windows but one of the electrodes is composed of reflective material instead of transparent, to allow EC device to work as a normal mirror when it is in its off-state, and a darkened mirror when it is in its on-state. It is introduced first by Gentex in 1982 [33]; these mirrors regularize reflections of flashing light from following vehicles at night, so enable the driver to see without discomfort.

2.2.3 Types of electrochromic devices

Electrochromic devices are classified into three major configurations: solution phase, hybrid structure, and battery-like devices [28], as clarified in Fig. 2.4. For solution and hybrid type ECDs, at least one electrode should be solution or gel-type electrolyte. they are called self-erasing types, since a continuous passage of current is needed to keep the colored state,

they are more appropriate to be used as a rear-view EC mirrors in cars. Otherwise, battery-like devices have a good memory effect under open circuit potential. Coloration of the two electrodes, in battery-like devices, complements one another, thus it shows their electrochromic superiority to the solution and hybrid types [41].

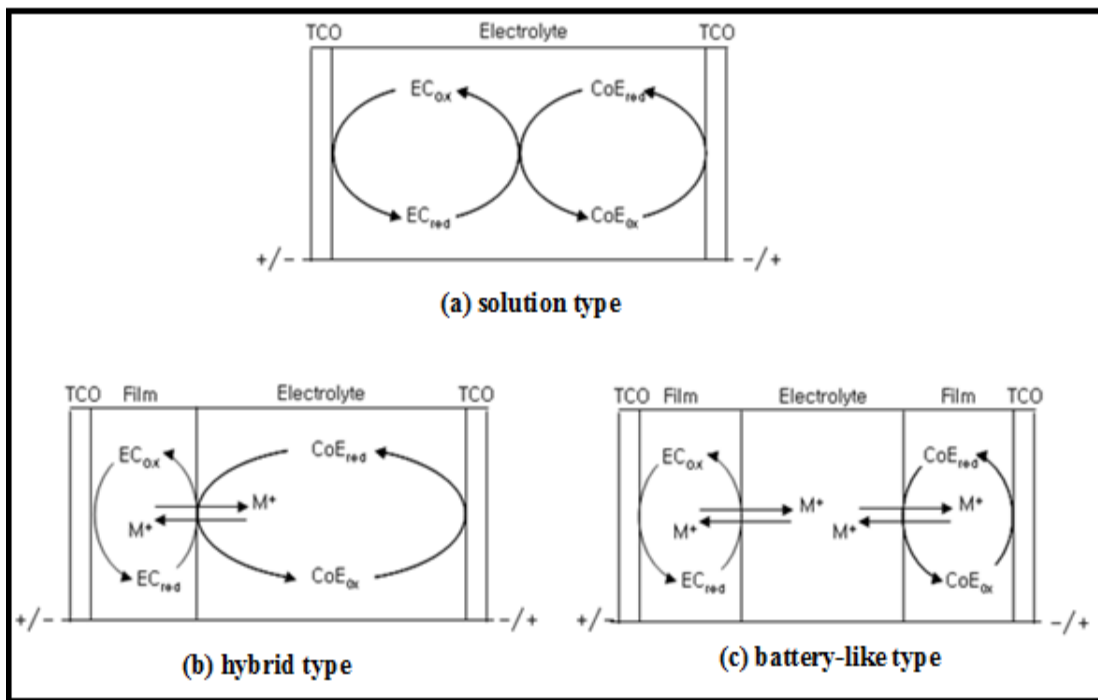


Fig (2. 4): Three different types of electrochromic devices (ECDs): (a) solution type, (b) hybrid type, and (c) battery-like type.

2.3 Background on tungsten and Tungsten oxide

2.3.1 Tungsten

Tungsten is a hard, grayish white, paramagnetic element, and uncommon metal under standard conditions when uncombined. Tungsten occurs in group 6 and period 6, with atomic number of 74, atomic mass of 183.84 g/mole [42], and electronic configuration $[Xe] 4f^{14}5d^46s^2$. the melting point

for tungsten is about 3422 °C, which is the highest melting points of all the elements, and the boiling point is about 5930 °C, it has also a remarkable high density which is 19.3 g/cm³. Tungsten has different oxidation numbers (0, 1⁺, 2⁺, 3⁺, 4⁺, 5⁺, and 6⁺), and it forms heavy alloys which have enormous applications, such as: rocket nozzles, automotive industries, and in military applications [43]. Tungsten combine with different elements as: Boron, Carbon, Silicon, Nitrogen, Phosphorous, Arsenic, Oxygen, Sulfur, Fluorine, Chlorine, Iodine, and Bromine, and these compounds often used in industrial catalysis, electrochromic devices, and ceramic glazes.

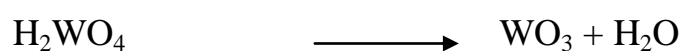
2.3.2 Tungsten oxide (WO₃)

WO₃ is a chemical compound containing oxygen and the transition metal tungsten. This n-type semiconductor has an intermediate band gap (2.7 eV), it appears as a yellow powder and has a molar mass of 231.84 g/mole, and its density is 7.16 g/cm³. WO₃ melting point is 1473 °C, while its boiling point is 1700 °C [44].

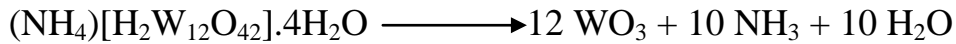
(a) Preparation

There are several ways to prepare Tungsten oxide, as:

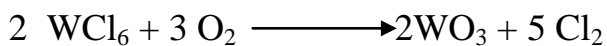
- Allowing CaWO₄ or scheelite to react with HCl to produce tungsten acid (H₂WO₄), this decomposes to WO₃ and water at high temperature.



- Annulment of ammonium paratungstate (APT) upon oxidizing conditions



- Dissolving WCl_6 powders in alcohols or in the presence of air, this result in oxidizing WCl_6 by bringing O_2 into the solution [45].



(b) Structures

Tungsten oxide is made from octahedrally WO_6 building blocks. In this structure, tungsten ions are located and surrounded by six oxygen ions, and each oxygen located between two tungsten ions (Fig. 2.5). In this stable structure, which is transparent in a thin film form, every oxygen ion is shared by two corner shaded blocks. Actually, single crystals of WO_3 exhibit a various crystallographic phase structures in different temperature ranges, it is triclinic from -50 to 17 °C, monoclinic from 17 to 330 °C, orthorhombic from 330 to 740 °C, and tetragonal above 740 °C. The room temperature stable form of WO_3 is Monoclinic. Monoclinic structure has the space group $\text{P}21/\text{n}$ with unit cell parameters: $a = 7.301$, $b = 7.539$, $c = 7.690$ Å and $\beta = 90.89^\circ$ [46, 47].

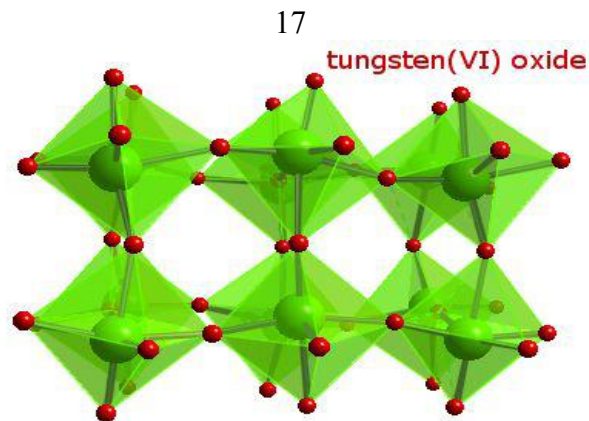


Fig. (2.5): monoclinic structure of Tungsten oxide (WO_3) at room temperature.

(c) Applications

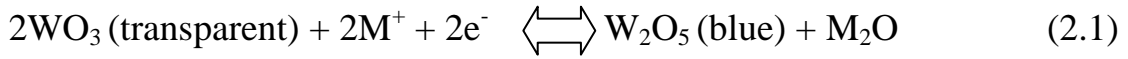
The interesting optical, electrical, and photocatalytic characteristics of WO_3 make them promising material for modern technological applications, thus it is used in several fields as in electrochromic devices, dye-sensitized solar cells, sensors, field emission, high temperature super conductor, and photo catalysis [48], it is also used to manufacture fireproofing fabrics, pigments in ceramic and paints, and to produce tungstate for x-ray screen phosphors.

2.4 Coloration mechanism of Tungsten oxide-based thin films

Tungsten oxide is the most favorable and excessively studied electrochromic material. A publication by Deb in 1969 showed that color centers could be created in thin films of Tungsten oxide by the addition of an electric field [49]. Therefore, its color switches from transparent to opaque (blue) as a result of a little applied voltage.

Various models have been proposed to demonstrate the electrochromic mechanism in WO_3 films [4, 7, 49-53]. Coloration from transparent case to

dark blue color follows by the injection of electrons and protons (or alkali ions) into the WO_3 film as in this reaction:



Where ($\text{M} = \text{H}, \text{Li}, \text{Na}, \text{etc.}$), Eq. (2.1) indicates that an electric field will help injected ions (M^+) crash some of the $\text{W}=\text{O}$ bonds and combine with O^{2-} to form M_2O . Consequently, this will induce W^{+5} states. An inverted electric field will break the $\text{M}-\text{O}$ bond and separate the M^+ ions from the film. Then the W^{+5} state will liberate an electron and return to the W^{+6} state. This operation can be described clearly in Fig. (2.6).

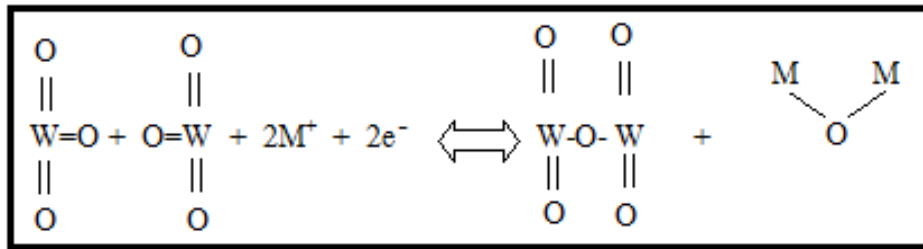


Fig. (2.6): The reduction of W^{+6} in WO_3 to a W^{+5} state and the oxidation of M^+ to form M_2O .

2.5 Electrochromic properties

2.5.1 Cyclic voltammetry (CV)

Cyclic voltammetry is a strong analytical method for studying electrode operation by applying continuous cyclic potential to working electrode [54]. In this case the voltage is swept linearly and periodically between two values (V_1, V_2) at given potential scan rate, V_1 and V_2 are sometimes called

the switching potentials; when the voltage reaches V_2 the scan voltage is reversed and the voltage is return to V_2 .

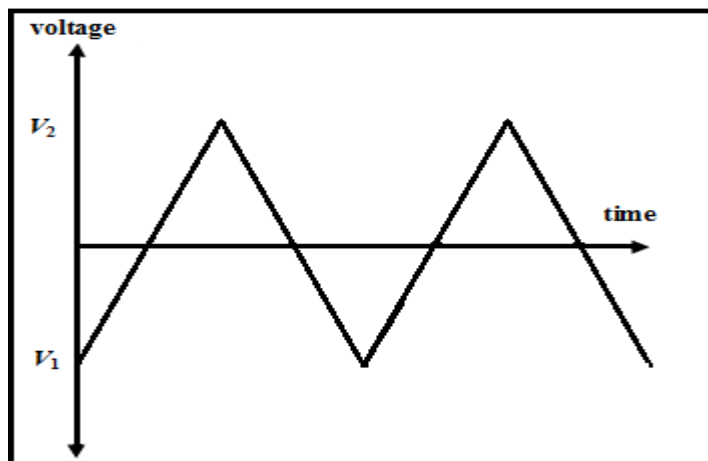


Fig. (2.7): Voltage swept during CV experiments.

Currents produced by the reduction and oxidation reactions at the working electrode are measured and drawn versus applied potential on a cyclic voltammograms. Fig. (2.8.a) shows the shape of ideal CV for a single electron transfer operation. Cyclic voltammograms are distinguished by peak potentials (E_p), at which the current reaches a local maximum or minimum, and the value of the peak current (i_p) at these points. When a redox reaction is 100% reversible, the measured CV has particular well defined properties:

1. The positions of peak voltage do not alter as a function of voltage scan rate, and the peak currents increases with increasing scan rate as appear in Fig. (2.8.b).
2. The ratio of the peak currents is equal to one

$$i_{pa}/i_{pc}=1 \quad (2.2)$$

Where, i_{pa} is the anodic peak current, and i_{pc} is the cathodic peak current. But, the ratio of peak currents can be significantly affected in irreversible reactions [55].

3. The peak currents are proportional to the square root of the scan rate.

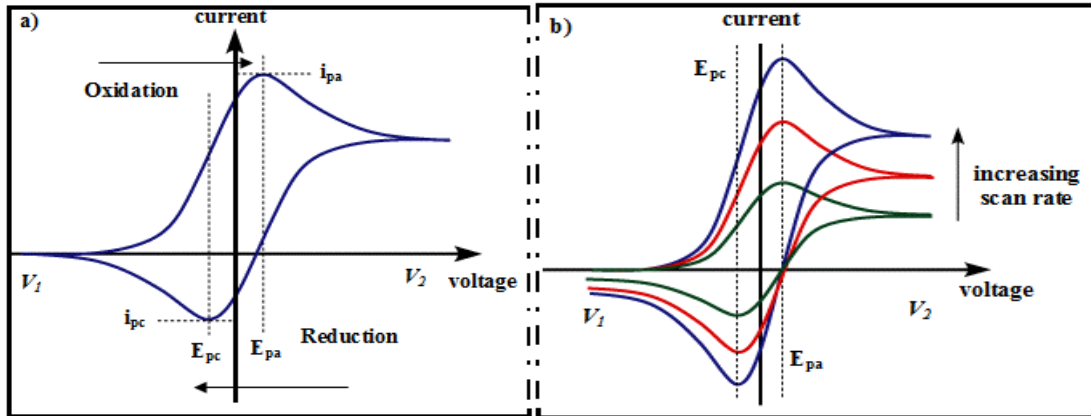


Fig. 2.8: A typical cyclic voltammograms recorded for a reversible single electrode transfer reaction a) at one scan rate b) at different scan rate.

CV consists of cycling the potential of an electrode that is immersed in an unmovable solution (no stirring), and gauge the obtained current. The working electrode potential is modified against a reference electrode like a saturated calomel electrode (SCE) or a silver chloride electrode (Ag/AgCl). For a reversible system, the peak current (i_p) is stated by the Randles-Sevcik equation which is:

$$i_p = (2.69 \times 10^5) n^{3/2} A D^{1/2} C \nu^{1/2} \quad (2.3)$$

Where i_p is peak current, n is the number of electrons used in the redox event, A is electrode area, D is diffusion coefficient, C is concentration of active metal ion in the electrolyte (mol cm^{-3}), and ν is scan rate [56]. As

appear from Eq. (2.3), i_p increases with $v^{1/2}$. A plot of i_p vs. $v^{1/2}$ is usually involved to find the Diffusion coefficient from the slope of this plot.

2.5.2 Chronoamperometry (CA)

Chronoamperometry is defined as an electrochemical mechanism through which the potential of the working electrode is stepped and the obtained current is plotted against time [57], as in Fig. (2.9). It is usually used for calculating switching times, which is the time needed for an electrochromic device to change from its color to its bleached state and vice versa.

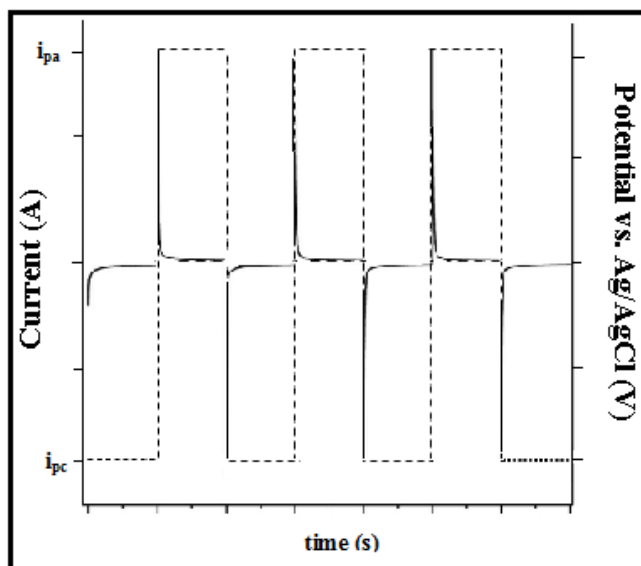


Fig. 2.9: Chronoamperometry curve showing current (—) response with applied potential (----).

Diffusion coefficient also can be calculated from Cottrell equation which clarifies the current-time reliance for linear diffusion control as in this relation [55]:

$$i = nFACD^{1/2} \pi^{-1/2} t^{-1/2} \quad (2.4)$$

Whereas: n = number of electrons transferred in unit reaction

F = Faraday's constant (96,500 C mol⁻¹)

A = electrode area (cm²)

D = diffusion coefficient (cm² s⁻¹)

C = concentration of active metal ion in the electrolyte (mol cm⁻³)

From the above relation it is appear that there is a linear relationship between the current and the 1/square root of time. A graph of i vs. $t^{-1/2}$ is usually referred to as the Cottrell plot. Diffusion coefficient could be determined from the slope of this plot.

2.6 Optical properties

An electrochromic device could be evaluated with its Absorbance, A , which is equal to change of optical density $\Delta OD(\lambda)$,

$$A = \Delta OD(\lambda) = \log T_b / T_c \quad (2.5)$$

Where, T_b and T_c represent transmitted light intensity in bleached and colored cases, respectively. Optical density change, $\Delta OD(\lambda)$, can also be expressed by [58],

$$\Delta OD(\lambda) = \eta Q = CE \cdot Q \quad (2.6)$$

Q is the injected electronic charge per unit area needed to switch the electrochromic thin film material from colored to bleached state. η indicates the coloration efficiency, which is also expressed as CE (cm²/C), and defined as the rate of the variation of the optical density to the injected charge as a function of unit area [59]. Therefore, CE is proportional to ΔOD and inversely proportionate to the quantity of electric charge per unit area, according to Eq. (2.6):

$$CE = \Delta OD(\lambda) / Q$$

An electrochromic device with high coloration efficiency provides big difference in transmittance with few amount of electric charge. The most representative inorganic thin film electrochromic substance as WO_3 and NiO have coloration efficiency (CE) of $\sim 40 \text{ cm}^2/\text{C}$, whereas organic electrochromic thin films, as PEDOT, show more than $100 \text{ cm}^2/\text{C}$ in CE [36]. Electrochromic devices are also evaluated according to their response time. Which is the time wanted for an electrochromic apparatus to change from its color to its bleached case and vice versa [60]. Electrochromic devices show lower response times than those for liquid crystal displays (LCDs). Another desirable property for long life cycle is the stability of the electrochromic devices, which is measured by the number of repetitive color-bleach cycles the device able to do without degradation. Preparing more stable electrochromic material is an obvious goal of all manufacturers, since it provides the consumer with a longer life electrochromic device.

2.7 Deposition technique of WO_3 -based thin films

Electrochromic WO_3 thin film can be prepared by many methods. The major methods are classified into physical, chemical, and electrochemical technique.

2.7.1 Physical Techniques

(a) Sputtering

Sputtering is defined as a momentum transfer operation in which atoms from a cathode/target are driven off by bombarding ions [61]. Sputtered atoms move until they hit a substrate, where they deposit to

form the required layer. The sputtering operation involves the creation of gas plasma (usually an inert gas, such as argon, in order to avoid any chemical reaction between the sputtered atoms and the sputtering gas) via applying a voltage between cathode and anode. Ions of the plasma are accelerated at the target by a large electric field. When the ions impact the target, atoms (or molecules) are ejected from the surface of the target to the plasma, wherever they get carried away and then deposited on the substrate. This kind of sputtering is called DC sputtering. Some implementations, as the deposition of nitrides and oxides, a reactive gas is inserted to argon, thus the deposited film is a chemical compound. This kind of sputtering is named as reactive sputtering. For effective momentum transport, the atomic weight of the sputtering gas should be near that of the target, thus for sputtering light elements neon is favored, whereas for weighty elements krypton or xenon are used. Sputtering is involved extremely in thin antireflection coatings on glass for optical implementations, in semiconductor industry to precipitate thin films of various materials in integrated circuit treatment, , and it is atypical method to deposit contact metals for thin-film transistors.

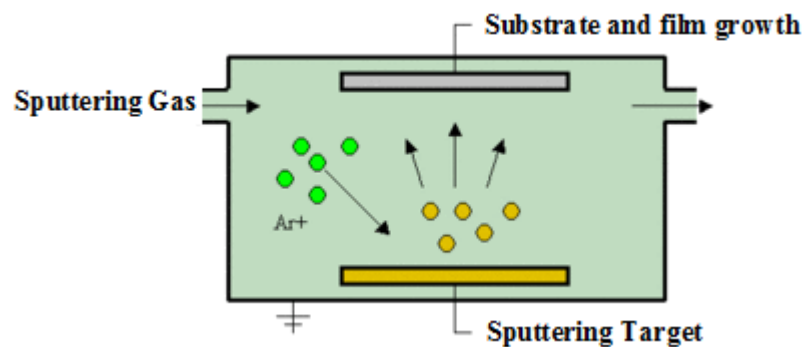


Fig. (2.10): Basic elements of sputtering system.

(b) Electron beam evaporation

A process of evaporation where a beam of electrons emitted in a way that it will heat and vaporize the material to be deposited. This technique occurs under a high vacuum to let molecules to transmitted freely in the chamber and thus compress on all surfaces including the substrate [62]. Fig. (2.11) illustrates schematic display of electron beam evaporation technique. At first, thermionic emission causes heating process of the hot filament. The hot filament will generate a beam of electrons that is excited as a result of heating. Then the beam of electrons heats the material that is to be deposited. This material is appeared in Fig. (2.11) as evaporant in water-cooled hearth. The material will be heated up to a boiling point, once the boiling point is reached, the molecules in the liquid (material evaporant) will shock and transmit energy to each other and hence the liquid would convert into vapor. Wherefore, the material evaporant can travel freely in the high vacuum area. Once the material evaporant is move, it could arrive to the substrate and link on it, which is the last step in this operation.

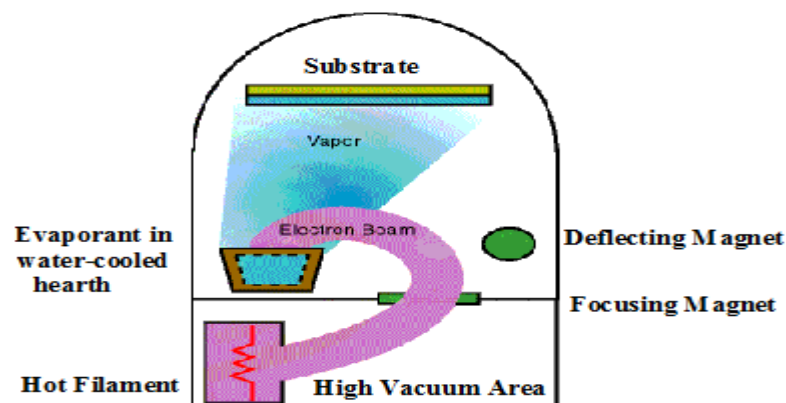


Fig. (2.11): A schematic shows of the electron beam evaporation process.

(c) The pulsed laser deposition technique (PLD)

Pulsed laser deposition is defined as a mechanism where a large power pulsed laser beam is condensed in a vacuum chamber to hit a target of the substance that is to be deposited. The process uses high power laser pulses (commonly $\sim 10^8 \text{ Wcm}^{-2}$) to melt, vaporize and ionize material from the surface of a target [63].

The detailed mechanisms of PLD are very complicated including the ablation operation of the target material by the laser irradiation, the creation of a plasma plume with huge energetic ions, electrons, and the crystalline accretion of the film itself on the heated substrate. The procedure of PLD can be split into four steps:

- Laser ablation of the target substance and production of a plasma
- Moving of the plasma
- Precipitation of the ablation material on the substrate
- Growth of the film on the substance surface

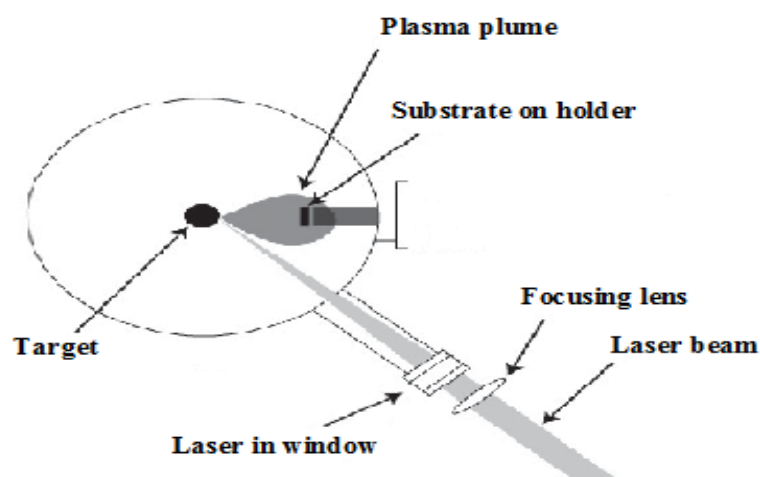


Fig (2. 12): A typical composition of a PLD technique chamber.

The main factors that affect deposition thickness and crystallinity are:

- The target material (structure, density).
- The laser energy
- Target and substrate separation.
- The gas kind and pressure in the chamber (Oxygen, Argon, etc.) [61].

2.7.2 Chemical Techniques

(a) Electrochemical Deposition (ECD)

Electro-deposition technique is defined as the process of manufacturing a coating on a cathodic plate electrode by the addition of electric current inside an electrolytic cell. This kind of deposition (coating) have some features, as [64]:

- Surface smoothness.
- Good performance of protection versus corrosion.
- Little environmental pollution.
- Ease of processing and thickness predominance.
- Ease of condition control as concentrations, pH and temperature.
- Big area manufacturing.
- Very low manufacturing cost.
- Agreement with a variety of substrates.

(b) Chemical Bath Deposition (CBD)

The Chemical bath deposition is a method used to deposit thin films and nanomaterial. This operation usually employs the simple immersion of a material into a solution having both a metal salt and a chalcogenide precursor [65]. Thus, this technique doesn't require expensive capital equipment; the only apparatus needed for CBD process are suitable solution containers and substrate mounting devices. CBD technique is simple, inexpensive, and safe method. It results in uniform, adherent, stable and hard films with good reproducibility via a relatively simple procedure.

(c) Sol-gel process

The sol-gel procedure is a many sided solution operation for preparing advanced materials, such as ceramics and organic-inorganic hybrids. “Sol-gel” word originated from “sol” means the forming of a colloidal suspension of solid particles of ions in a solvent, and “gel” is a semi rigid mass result from solvent evaporation and particles joining in the form of a continuous network. Implementations for sol-gel method contain high-strength ceramics, catalysts, protective coatings, wave-guides, piezoelectric devices, superconductors, lenses, formation of nanoparticles and insulating materials; it can be involved to make fibers, microspheres, thin films, fine powders and monoliths. Sol-gel method attracts particular attention as a result of its features [66], as:

- Inexpensive technique
- low temperature method
- Avoid pollution during work

- Create very fine powders
- High chemical homogeneity
- Enable controlling the size and morphology of particles
- For doped sol-gel material; it preserves the chemical and physical properties of the dopants.

The disadvantages of Sol-gel processing include [67]:

- Stress by shrinkage of the gel upon drying
- Thick coatings are only achieved by adding organic components, or by controlling the pore size.
- Limited life time of the sol.

The ideal steps used in sol-gel operation are presented in the schematic show below (Fig. 2.13).

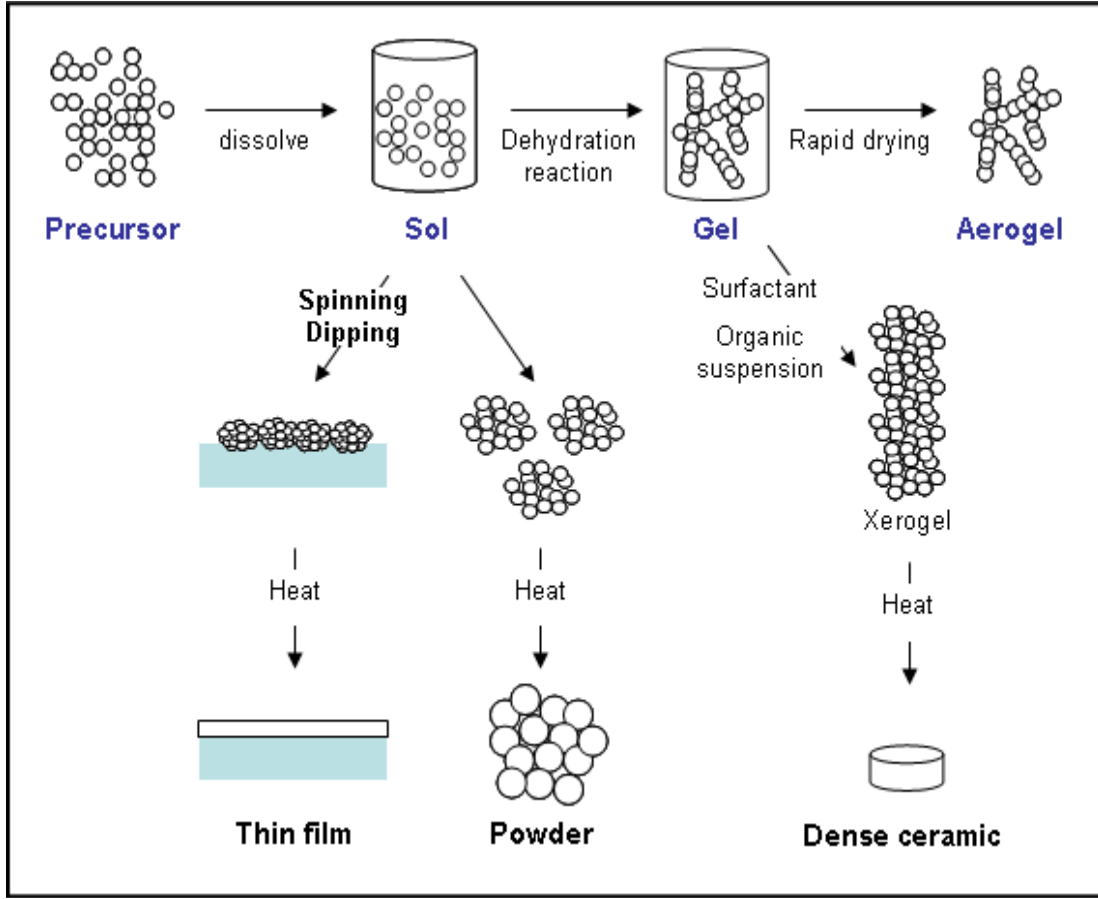


Fig. (2. 13): Schematic show of sol-gel process to synthesize nanomaterials, thin films, and ceramics.

(d) Spin Coating (SC)

Spin coating is a method used to deposit regular thin films to flat substrates [67]. A coating process involving spin coater or spinner is clarified in Fig. (2.14). usually a few amount of coating material is added on the center of the substrate that is either spinning at low speed or not spinning at all. After that, the substrate is revolved at high speed to disseminate the coating material by centrifugal force. An instrument involved for spin coating is named a spinner or spin coater.

Rotation is lasted whereas the fluid spins off the edges of the substrate, till the required thickness of the film is done. The used solvent is generally volatile, and evaporates. Thus, the higher the angular speed of spinning, the thinner the film. However, viscosity and concentration of the solution and the solvent affect the thickness of the film.

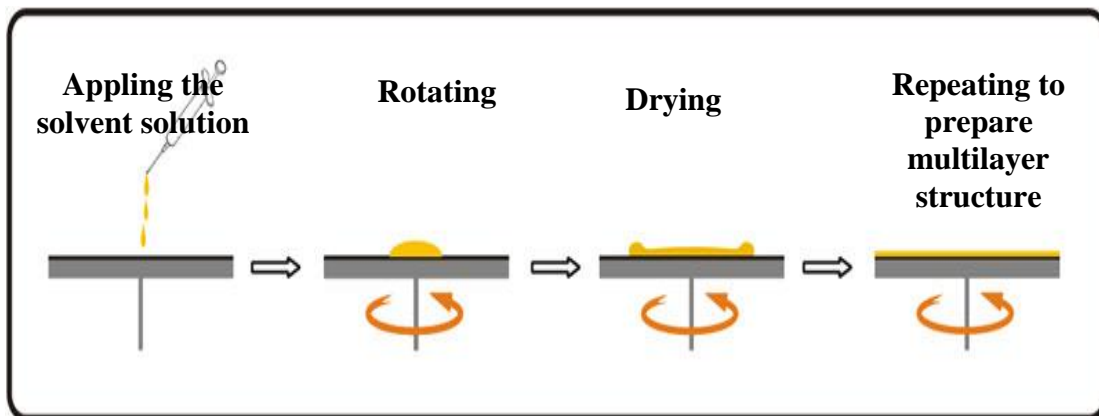


Fig. (2. 14): A spin coating process.

Spin coating is applied in microfabrication of oxide layers involving sol-gel precursors, while it may be used to produce regular thin films with nanoscale thicknesses, it is involved extremely in photolithography, to precipitate layers of photoresist around 1 micrometre thick.

(e) Dip Coating

Dip coating method is a method where the coated substrate is immersed in a liquid and then withdrawn with a determined withdrawal speed at known temperature and atmospheric conditions [68]. Fig. (2.15) represents the substrate dipping into the coating solution.

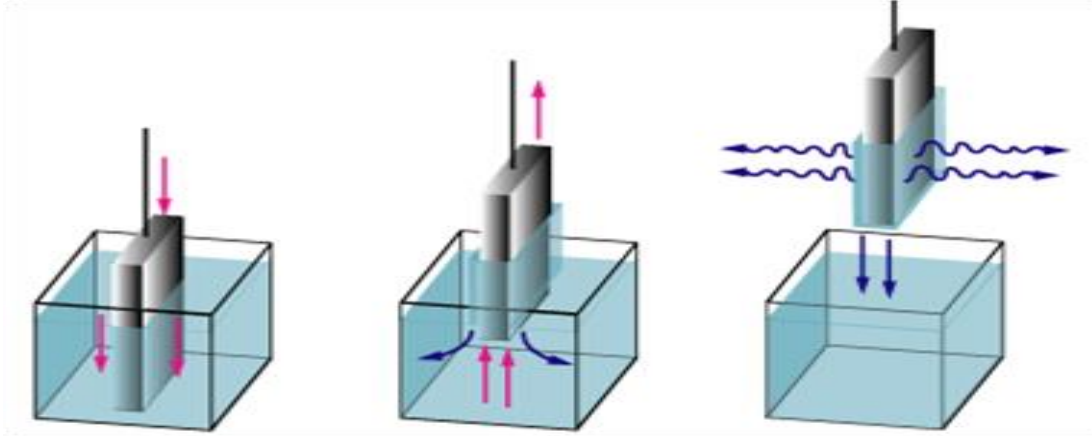


Fig (2. 15): Schematic presentation of the stages of the dip coating process.

The dip coating process can be divided into three main stages:

- **Immersion:** The substrate is dropped at a constant speed in solution of the coating material.
- **Wet layer formation:** The substrate has kept in the solution for some time. While the substrate is leaving the solution, thin layer precipitate itself on it. Then, the withdrawing is done at a fixed speed. The speed determines the thickness of the coating (faster withdrawal gives thicker coating material), and any excess liquid will drain from the surface.
- **Evaporation:** The solvent vaporize from the liquid, forming the thin layer.

Chapter Three
Experimental Work

Chapter Three

Experimental Work

3.1 Materials and film preparation

3.1.1 Chemicals and Solvents

Chemical materials are purchased in its pure form, from different companies:

- 1) Tungsten (VI) chloride (WCl_6) and Titanium (II) Chloride (TiCl_2) were purchased from Sigma-Aldrich.
- 2) Zinc Chloride (ZnCl_2) is from Chem. Samuel.
- 3) Sulfuric acid (H_2SO_4) is from Biolab.
- 4) Other materials such as ethanol, methanol, acetate, glycerol and hydrochloric acid (HCl) are self-packing locally.
- 5) Fluorine-doped tin dioxide on glass (FTO/ glass) samples which used as substrates. They were bought from Sigma-Aldrich.

3.1.2 Preparation of WO_3 based films using sol-gel dip coating technique

a) Substrate Cleaning Process

FTO/glass substrate which has dimensions of $5 \times 1 \text{ cm}^2$ was prepared to settle WO_3 -based electrochromic films. So as to gain good adherence and uniformity for the films, it is needful to use pre-cleaned substrates, The FTO/glass substrate cleaning procedure was as follows:

- 1) Mopping FTO with acetate to remove any gluey material on it.
- 2) Washing with liquinox soap in order to clean any dusts.
- 3) Washing with deionized water to eliminate soap.
- 4) Washing with methanol to melt any oily attachments.
- 5) Vibrate in dilute HCl (10%) for 5 seconds to dissolve any uncleaned attaches.
- 6) Washing with deionized water once again
- 7) After that, the substrate left to dry in air to be utilized in sol-gel /dip- coating process.

b) Sol-gel solution preparation

Two types of WO_3 -based electrochromic films (WO_3 doped with Ti and WO_3 doped with both Ti and Zn) were prepared by sol-gel solutions. For the two compositions mentioned above, two different solutions were prepared.

1) Sol-gel solution for WO_3 doped with Ti ($\text{WO}_3\text{:Ti}$) films

In its film form, after annealing, titanium was assumed to compensate W in the WO_3 structure according to " $\text{W}_{1-x}\text{Ti}_x\text{O}_3$ ". This assumption is due to the fact that atomic radii close to each other [69]. Ti concentration in the nominal composition of $\text{W}_{1-x}\text{Ti}_x\text{O}_3$ varies from atomic concentration (x) equals 0.0 to 0.3 in steps of 0.05. For different atomic concentration of Ti, TiCl_2 and WCl_6 , with appropriate molar concentration, were dissolved in 10 ml of ethanol and 1 ml of glycerol (used as binding material in sol-gel solution).

This solution was stirred continually with repeated sonicating and stirring for 2h. The color of the solution differs quickly from yellow after preparation to blue (as in Fig. 3.1). In order to prepare 0.4 M sol-gel solution of $W_{1-x}Ti_xO_3$ see table 3.1.

Table (3.1): list of different nominal film composition, Tungsten (VI) chloride mass, and Titanium (II) Chloride mass, solutions were prepared in 10 ml of ethanol and 1 ml of glycerol.

Sample no.	Nominal composition	Tungsten (VI) chloride (gm)	Titanium (II) Chloride (gm)
1	WO_3	1.745	0
2	$W_{0.95}Ti_{0.05}O$	1.658	0.026
3	$W_{0.90}Ti_{0.10}O$	1.570	0.052
4	$W_{0.85}Ti_{0.15}O$	1.483	0.078
5	$W_{0.80}Ti_{0.20}O$	1.394	0.105
6	$W_{0.75}Ti_{0.25}O$	1.309	0.131
7	$W_{0.70}Ti_{0.30}O$	1.221	0.157

2) Sol-gel solution for WO_3 co-doped with Ti and Zn

(WO_3 :Ti:Zn) films

Zinc dopant was added to compensate Ti atom in the WO_3 amorphous structure. The structure formula is assumed to be " $W_{1-x}Ti_{x-y}Zn_yO$ " after annealing the films. Similar formula was assumed by Dae-hoon park for Zn dopant that compensate Ti in the NiO:Ti films [28]. For the films of WO_3 doped with Ti alone (previously prepared), the best sample, in term of electrochromic properties, was found for the WO_3 films that contains molar concentration ratio of 0.05 of Ti ($W_{0.95}Ti_{0.05}O$). Hence for the WO_3 co-doped with Ti and Zn, we will maintain the W molar

concentration ratio to 0.95. Accordingly, the structure formula can be written as “ $W_{0.95}Ti_{0.05-y}Zn_yO$ ”. 0.4 M sol-gel solution of $W_{0.95}Ti_{0.05-y}Zn_yO$ was prepared in 10 ml ethanol and 1 ml glycerol; with Zn molar concentration varies from 0.0 - 0.05 in steps of 0.01 (see table 3.2). The sol-gel was prepared by adding $ZnCl_2$ to the powder mixture in $W_{0.95}Ti_{0.05}O$ solution, and then completes preparing the solution as done previously.

Table (3.2): list of intended structure, Titanium (II) Chloride mass, and Zinc (II) chloride mass used in the sol-gel preparation. All sol-gel solutions contain 1.658 gm of Tungsten (VI) chloride.

Sample no.	Composition	Titanium (II) Chloride (gm)	Zinc (II) Chloride (gm)
1	$W_{0.95}Ti_{0.05}O$	0.026	0
2	$W_{0.95}Ti_{0.04}Zn_{0.01}O$	0.021	0.006
3	$W_{0.95}Ti_{0.03}Zn_{0.02}O$	0.016	0.012
4	$W_{0.95}Ti_{0.02}Zn_{0.03}O$	0.011	0.018
5	$W_{0.95}Ti_{0.01}Zn_{0.04}O$	0.005	0.024
6	$W_{0.95}Zn_{0.05}O$	0	0.030



Fig. (3.1): Steps of preparing sol-gel solution: (a) weighting, (b) stirring, (c) sonificating, (d) the color change of the solution from yellow to blue.

c) Dip-Coating Process

The produced sol-gel solutions were deposited on the pre-cleaned FTO/Glass substrate using dip coating process [68].

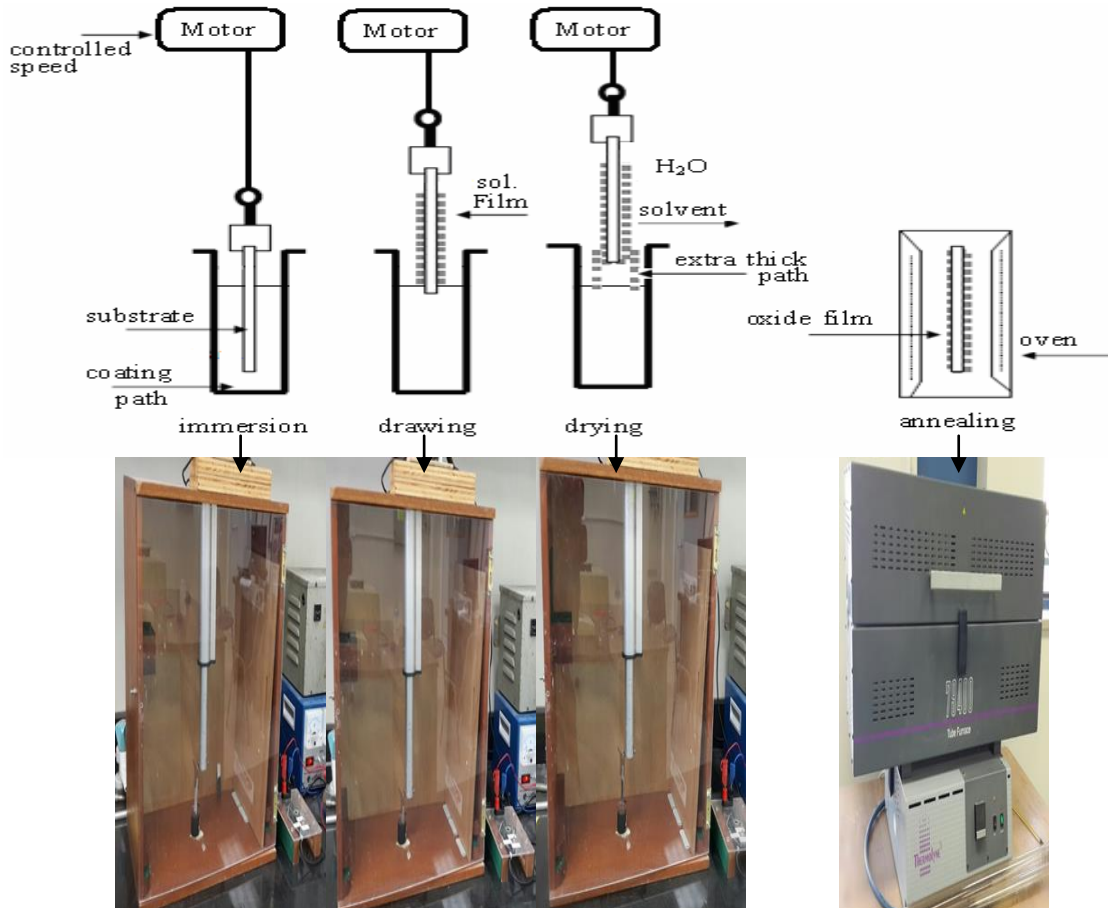


Fig (3.2): Procedure of WO_3 -based films deposition by dip coating process.

The steps of dip coating operation for WO_3 -based films is appeared in Figure 3.2 and abbreviated as follows:

- 1) Dipping cleaned FTO/glass substrate in the prepared sol-gel solution with a speed of 0.61 mm/s. Observe that part of the substrate was not immersed in solution for electrical contact with FTO.
- 2) The substrate left pendent in the solution for 10 min to get good exposure of the substrate to film.

- 3) Withdraw the FTO/Glass/film with speed of 0.61 mm/s
- 4) The FTO/Glass/film was remained above the sol-gel beaker, for 10 min. To allow homogeneous film formation, to drop any excess thick parts from the film surface, and to vaporize unwanted solvents.
- 5) The slides were stayed for one day under air to dry.
- 6) Samples were annealed at 350°C under air into the oven for 1.5 hours.

3.2 Measurements

3.2.1 Cyclic voltammetry (CV)

The cyclic voltammetry test were done using three electrodes electrochemical cell which presented in Fig. 3.3, it includes 0.25 M H₂SO₄ aqueous solution as an electrolyte (to check the stability of the prepared films in this strong acid). The WO₃ based electrochemical films precipitate on FTO/Glass were involved as working electrode (WE), the silver/silver chloride (Ag/AgCl) was involved in the cell as reference electrode (RE), and the platinum was involved as counter electrode (CE).

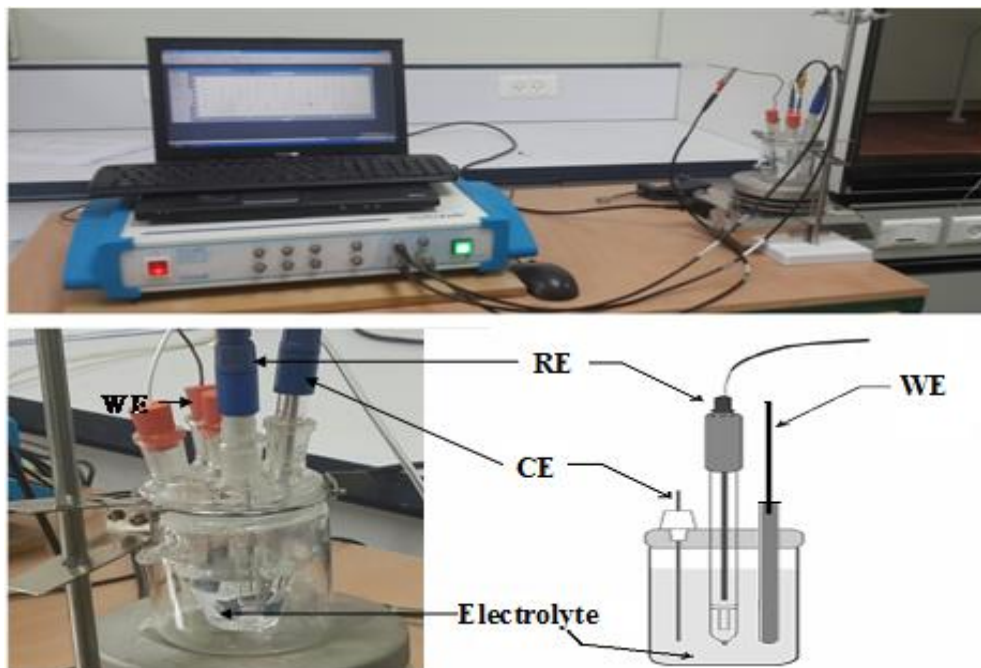


Fig. (3.3): A potentiostat device with three electrodes electrochemical cell.

a) $\text{WO}_3\text{:Ti}$ films

Cyclic voltammetry (CV) measurements were achieved, at room temperature, using the PGZ402 Universal Potentiostat. The potential switches between -800 and 500 mV, against Ag/AgCl reference electrode, at a scan rate of 100 mV/s (unless the curve that study the influence of scan rate on CV behavior). For every electrochromic film, 10 cycles have been registered. During all over CV measurements, the film area immersed in the electrolyte was kept to be $\sim 1 \text{ cm}^2$.

b) $\text{WO}_3\text{:Ti:Zn}$ films

To compare results of our two film types, CV measurements for co-doped films ($\text{WO}_3\text{:Ti:Zn}$) was done exactly as mentioned before for single doped film ($\text{WO}_3\text{:Ti}$).

3.2.2 Chronoamperometry (CA)

Chronoamperometry (CA) measurements were achieved, at room temperature, using the PGZ402 Universal Potentiostat. The potential varied

between -0.5 V and 0.5 V, against Ag/AgCl reference electrode with 10 s for each potential, the potential cycles varied between 1 and 10 cycles for each electrochromic film. The film area which was immersed in the electrolyte was kept $\sim 1 \text{ cm}^2$. CA measurements were done for all $\text{WO}_3\text{:Ti}$ and $\text{WO}_3\text{:Ti:Zn}$ films.

3.2.3 Transmittance

The transmission of light using single wavelength was done using Shimadzu UV-3101PC UV-Vis-NIR scanning spectrophotometer and recorded against time. Moreover, the transmittance, of the best film in WO_3 doped with Ti and WO_3 co-doped with Ti and Zn, during CA measurements (coloring and bleaching), was performed at a wavelengths of 633 nm.

Chapter Four

Results and Discussion

Chapter Four

Results and Discussion

Nano-particles of WO_3 semiconducting electrochromic thin films, doped by Ti and/or Zn, have been prepared. The effects of doping and co-doping, on prepared films characteristics (electrochromic and optical), have been studied involving different measuring techniques listed below:

- 1- Cyclic Voltammetry (CV).
- 2- Chronoamperometry (CA).
- 3- Optical transmission Spectra.

4.1 Tungsten oxide doped with Titanium ($\text{WO}_3\text{:Ti}$) thin films

In previous studies, researchers try to enhance the electrochromic properties of Tungsten oxide, either by using different preparation mechanism, using different electrolyte, or by doping WO_3 with various dopants [16-18]. The later procedure found to highly enhance electrochromic, optical, structural, and adhesion to substrate electrolytes [19-23]. 0.4 M sol-gel solution of $\text{W}_{1-x}\text{Ti}_x\text{O}_3$ was prepared in chemistry lab (see section 3.1.2) under ambient conditions, and deposited onto FTO/glass substrate. After dipping, the films were annealed at 350° for 1.5 hours.

4.1.1 Cyclic Voltammetry (CV)

Cyclic voltammograms was measured for $\text{WO}_3\text{:Ti}$ in 0.25 M H_2SO_4 electrolyte. The potential was cycled between -800 and 500 mV, against Ag/AgCl reference electrode, at a scan rate (v) of 100 mV/s. CV experiments have been done for prepared WO_3 films doped with different

Ti concentrations ($W_{1-x}Ti_xO_3$). The concentrations range between 0-30 % in steps of 5 % (Fig. 4.1).

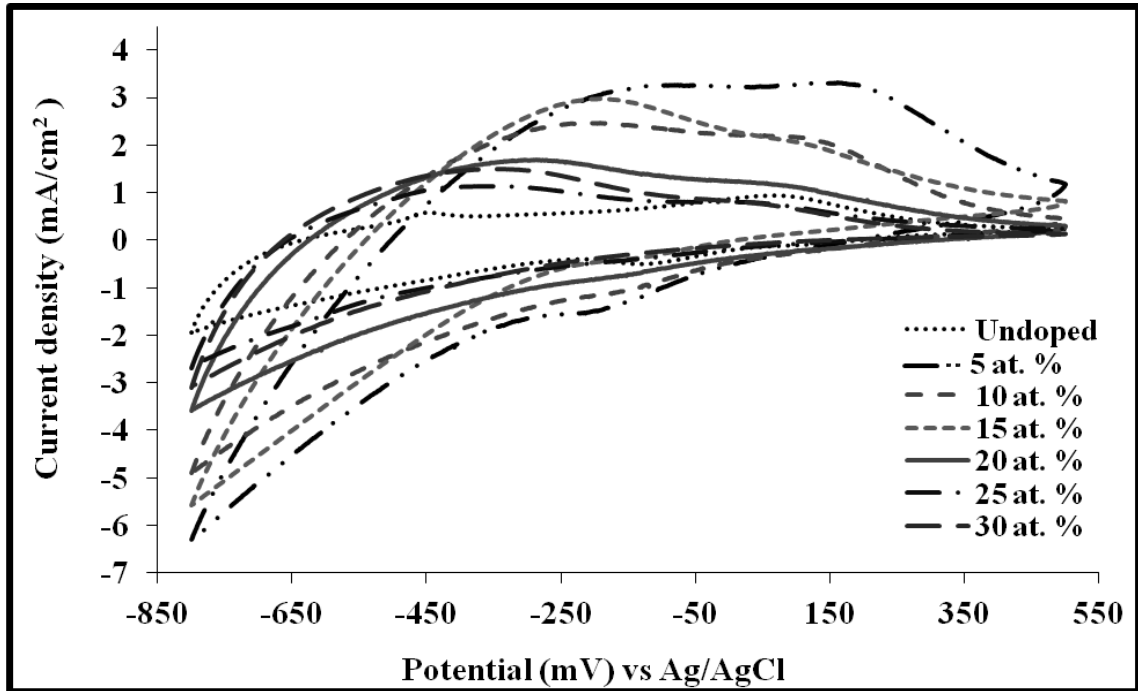


Fig. (4.1): Cyclic voltammetry measurements of the undoped and 5, 10, 15, 20, 25, and 30 at. % Ti doped WO_3 films at the scan rate of 100 mV/s.

The coloration and bleaching process were noted during CV measurements. The resulting current density is anodic peak current density (J_{pa}) associated with the bleaching process and cathodic peak current density (J_{pc}) related with the film coloring operation. During the coloration mechanism, which is in negative potential of the scan, the films have altered their color into blue, indicating the oxide reduction due to the intercalation of H^+ ions. After the reversal of the potential, the anodic current begins into its bleaching process. This refers to the electrochemical reaction presented in eq. (2.1).

As we can noticed, the anodic peak potential position changes with changing Ti atomic concentration, at Ti concentration of 5%, the anodic peak potential increases above the peak position of WO_3 alone (0% of Ti). However, for Ti concentration above 5%, the peak position was observed to be lower than that for 5% of Ti. Also, as noticed in Fig.(4.2.a and 4.2.b), the current densities (J_{pa} and J_{pc}) were observed to have the highest values for Ti concentration of 5% at.. This is due to the fact that Ti was totally inserted within the WO_3 since WO_3 has solubility limit of Ti on to its structure ranges between 0-6%, for higher Ti concentration (10%), other phases related to insulating Ti compounds like, TiO_2 , may occur [23]. This describes the decrease in current density values for Ti concentration above 10% at. Hence, WO_3 doped with Ti of 5% at. is considered to have only one phase related to WO_3 and consequently, it will have best electrochromic properties.

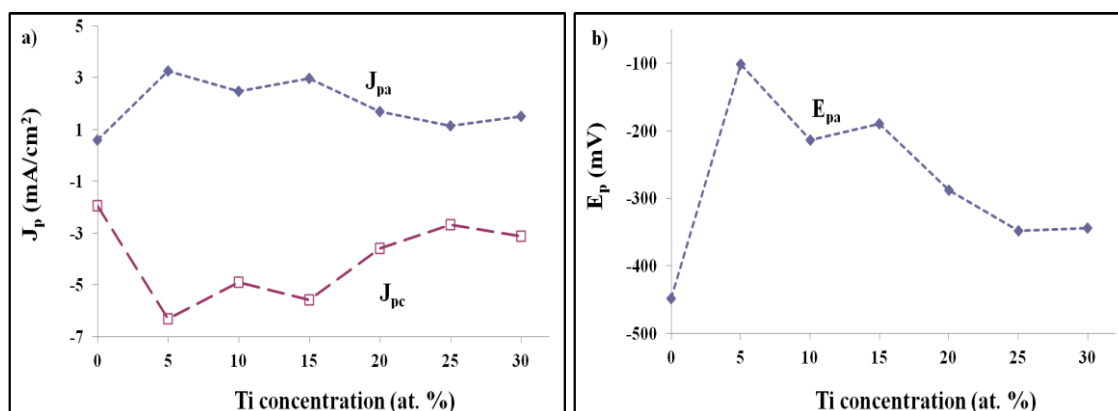


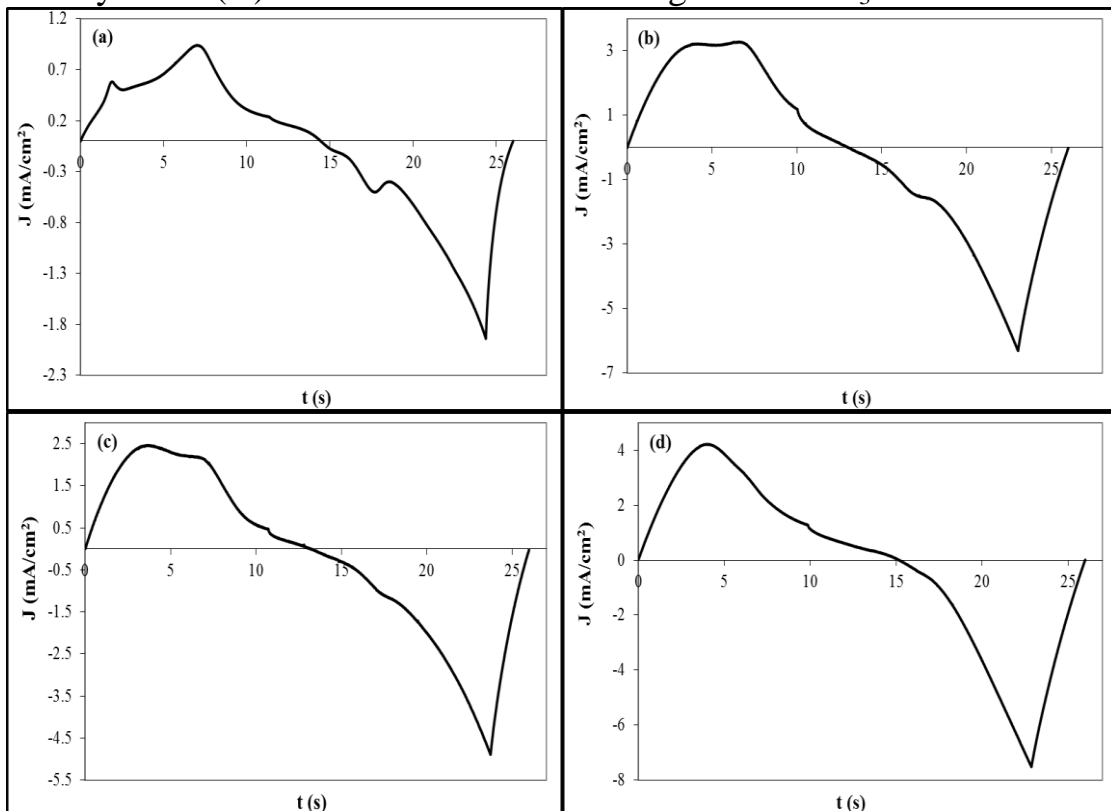
Fig. (4.2): Dependence of (a) peak current density (J_{pa} and J_{pc}), and (b) anodic peak potential (E_{pa}) on the Ti concentration.

For different Ti at. concentrations within WO_3 crystal, the current density (J) in the CV measurements was plotted versus time (t). From these graphs

(presented in Fig. 4.3), one can deduce the anodic charge density Q_a (charge density associated with positive current density $+J$) and the cathodic charge density Q_c (charge density associated with negative current density $-J$). The charge density can be calculated by integrating the J-t graph, according to:

$$Q = \int J dt \quad [4.1]$$

In general, as noticed before (Fig. 4.2.a) in CV measurements, the anodic current density ($+J$) peak has higher value for $WO_3:Ti$ films compared to WO_3 film. This indicates an increase in the anodic charge density Q_a injected in the layer, during bleaching of the layer (change from full coloration to full transparent). During coloration, the cathodic current density value ($-J$) was also observed to be higher for $WO_3:Ti$ films.



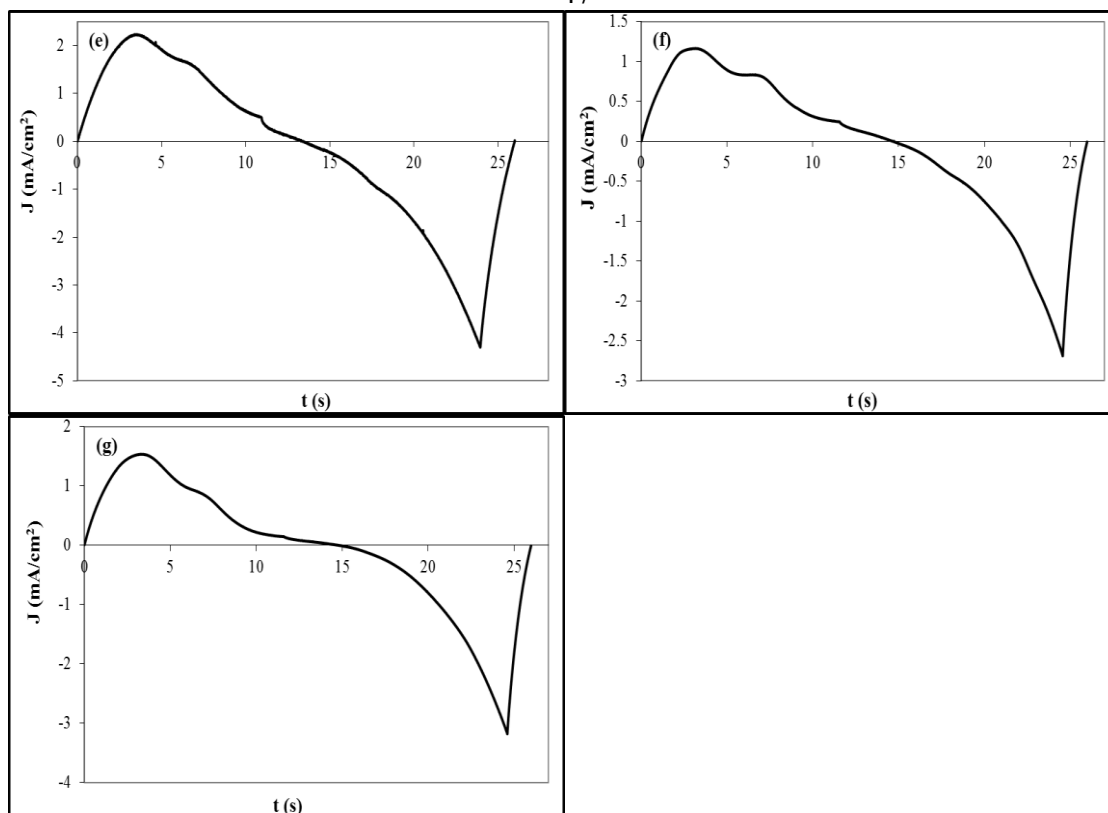


Fig. (4.3): Current density with time for WO₃:Ti with different Ti molar concentrations: a) WO₃, b) W_{0.95}Ti_{0.05}O₃, c) W_{0.90}Ti_{0.10}O₃ d) W_{0.85}Ti_{0.15}O₃, e) W_{0.80}Ti_{0.20}O₃, f) W_{0.75}Ti_{0.25}O₃, g) W_{0.70}Ti_{0.30}O₃. Experiment was performed at a scan rate 100 mV/s.

Typically, for fully reversible electrochromic process, for a given CV cycle, the ratio of the peak charges (Q_a and Q_c) is equal to one ($Q_a/Q_c=1$). In our experiments, Q_c was always observed to have slightly higher value than Q_a . This is due to quasi reversible reaction; results from slow electron exchange of the redox species with the working electrode. The calculated Q_a , Q_c and Q_a/Q_c for cycled WO₃:Ti films are presented in table 4.1. Not that the response time presented in the table was deduced from chronoamperometry experiments that will be described later.

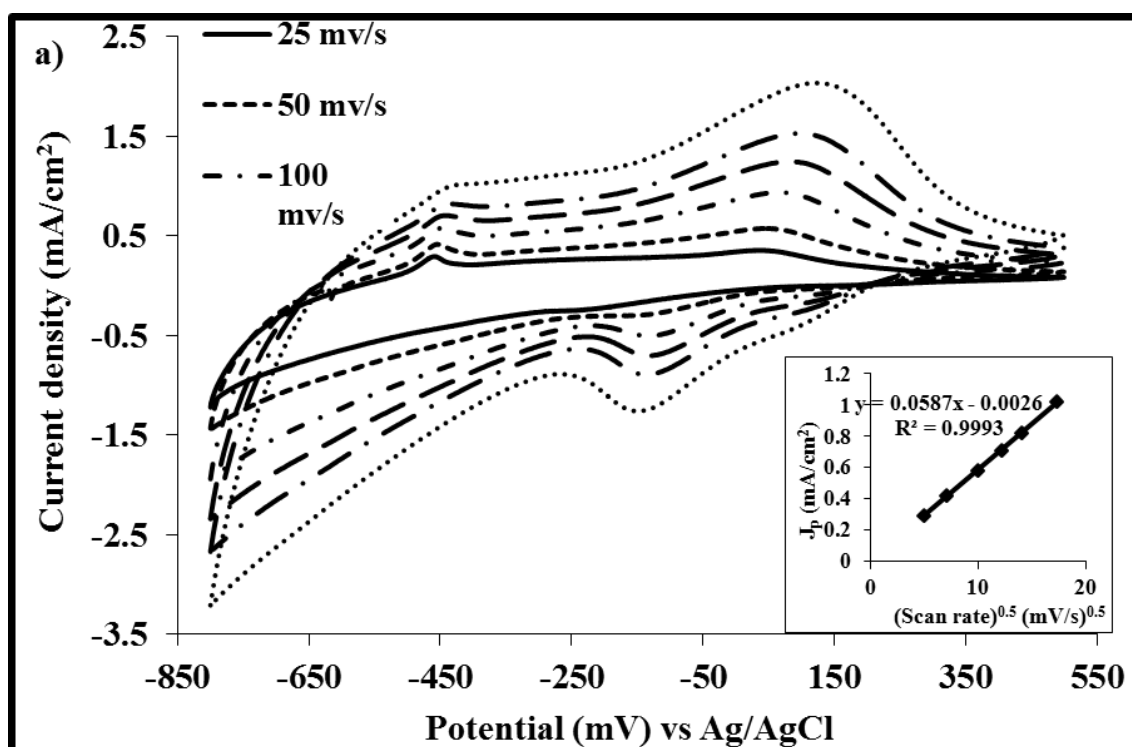
Table (4.1): The electrochromic properties for WO₃ doped with different molar concentration of Ti.

Sample Composition	Q _a (mC/cm ²)	Q _c (mC/cm ²)	Q _a /Q _c	Response Time	
				t _b (s)	t _c (s)
WO ₃	6.43	8.08	0.80	3	5.3
W _{0.95} Ti _{0.05} O ₃	21.59	24.77	0.87	5.6	4.4
W _{0.90} Ti _{0.10} O ₃	18.26	22.48	0.81	4.5	5.7
W _{0.85} Ti _{0.15} O ₃	28.57	33.05	0.86	3.7	4.1
W _{0.80} Ti _{0.20} O ₃	15.97	19.29	0.83	2.9	3.8
W _{0.75} Ti _{0.25} O ₃	8.33	10.20	0.82	2.5	3.5
W _{0.70} Ti _{0.30} O ₃	9.74	11.44	0.85	1.1	2.2

The ratio Q_a/Q_c is higher for WO₃ doped with Ti films than that of WO₃ alone. This points that the WO₃:Ti films have better electrochemical reversible reaction, indicating it may has better electrochromic properties. Between Ti doped WO₃, the ratio Q_a/Q_c was found to be the highest for WO₃:Ti with titanium contents of 5%. Hence, we can deduce that this film have the best electrochromic properties in term of electrochemical reversibility; since it is the closest to one. This is may be attributed to the surface nature of 5% Ti doped WO₃ that open up more channels for the charge insertion / de-insertion during the reduction / oxidation process [23]. To compare between WO₃ and doped WO₃, CV measurements at variable scan rates for WO₃ and W_{0.95}Ti_{0.05}O₃ films have been performed and are presented in Fig. 4.4 *a* and *b*, respectively. As expected, for both types of films, the magnitudes of both anodic and cathodic peak current densities increases with increasing scan rates. This increment in current densities is due to the fact that at faster voltage scan rates, the charge passed per unit

time is greater, which results in an increment in peak current density; the current is defined as the charge passed per unit time.

In the case of WO_3 film, the maximum current observed at scan rate (ν) = 300 mV/s is $J_{\text{pa}} = 2.04 \text{ mA/cm}^2$. While for $\text{W}_{0.95}\text{Ti}_{0.05}\text{O}_3$ film, $J_{\text{pa}} = 4.17 \text{ mA/cm}^2$ for same scan rate. This revealed that insertion and extraction of H^+ ions is enhanced in WO_3 film doped with Ti ($\text{W}_{0.95}\text{Ti}_{0.05}\text{O}_3$). The peak potential $E_{\text{p,a}}$ is appeared to be shifted toward higher potentials with increasing scan rate, this predicts that the process is quasi reversible. The reliance of J_{pa} against square root of the scan rate, illustrated in the inset of Fig. 4.4 (a) and (b). For both films, the graphs show a linear behavior.



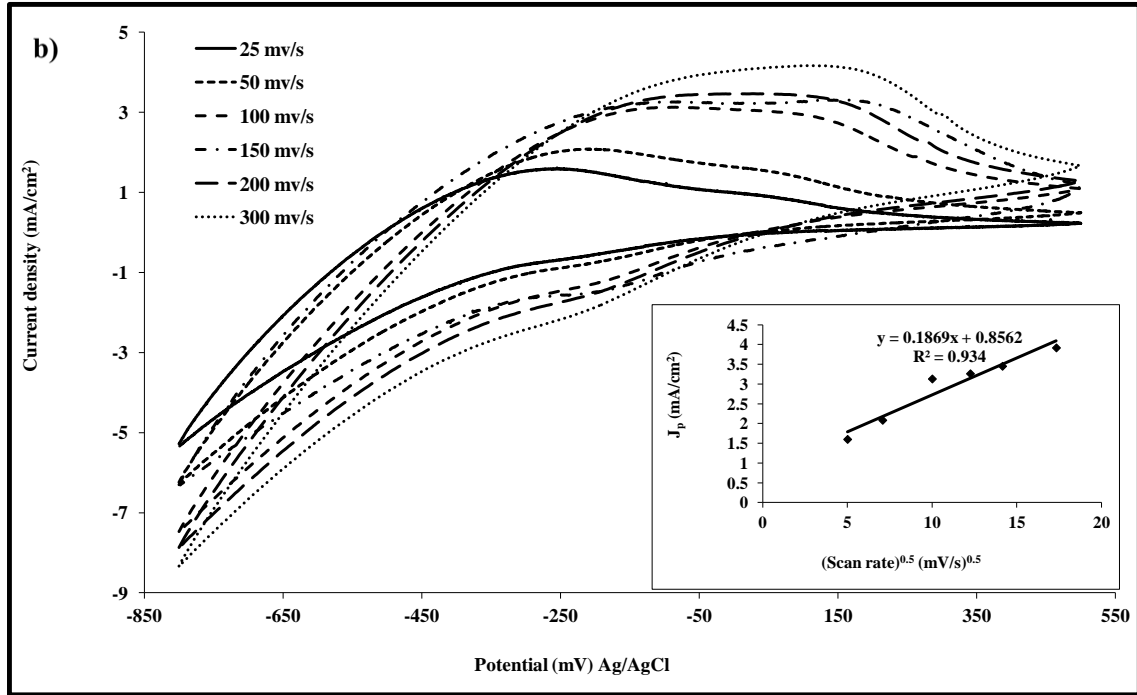


Fig. (4.4): Cyclic voltammety measurements for (a) WO_3 film (b) $\text{W}_{0.95}\text{Ti}_{0.05}\text{O}_3$ film at different scan rates. The inset shows the reliance of J_{pa} against square root of the scan rate.

The extent of insertion and extraction of H^+ ions can be studied by calculating the effective diffusion coefficient (D_i), which could be calculated from the oxidation peak current dependence on square root of the potential scan rate ν , rearrangement of eq. 2.3 results in:

$$D_i = 0.1382 \cdot 10^{-10} \text{ n}^{-3} \text{ C}^{-2} (\delta J_p / \delta \nu^{1/2})^2 \quad [4.2]$$

Where, δJ_p and $\delta \nu^{1/2}$ represent the slope of line in the inset graph.

Table (4.2) shows the scan rate induced variations in peak current density and diffusion coefficient values of WO_3 and $\text{W}_{0.95}\text{Ti}_{0.05}\text{O}_3$ films cycled in 0.25 M H_2SO_4 electrolyte solution.

Table (4.2): Calculation of diffusion coefficient using Randles-Sevcik equation.

Sample	Scan Rate (mV/s)	Peak Current Density (mA/cm ²)	Diffusion Coefficient (cm ² /s)	D* (cm ² /s)
WO ₃	25	0.29	4.81E-11	
	50	0.42	4.86E-11	
	100	0.58	4.69E-11	
	150	0.71	4.64E-11	
	200	0.82	4.71E-11	
	300	1.02	4.86E-11	
				4.80E-11
W _{0.95} Ti _{0.05} O ₃	25	1.60	1.42E-09	
	50	2.08	1.21E-09	
	100	3.13	1.36E-09	
	150	3.26	9.86E-10	
	200	3.45	8.29E-10	
	300	3.92	7.12E-10	
				4.87E-10

D* was calculated using the slope of J_p vs. $v^{1/2}$ plot in the inset of Fig. (4.4) For WO₃ film the diffusion coefficient generally increases with increasing scan rate, as found previously for WO₃ materials [70, 71], while the diffusion coefficient of the composite material (W_{0.95}Ti_{0.05}O₃ film), generally decreases with increasing scan rate [70]. The average of diffusion coefficients calculated at all scan rates and the value calculated using the slope of J_p vs. $v^{1/2}$ plot, are slightly different but follow the same trend. However, it is clear that W_{0.95}Ti_{0.05}O₃ film has larger diffusion coefficient than that of WO₃ alone, because of larger value of the ratio between peak current density and square root of the scan rate in case of W_{0.95}Ti_{0.05}O₃ film (larger diffusion coefficient also explain why Q_a in table 4.1 has larger value in case of W_{0.95}Ti_{0.05}O₃ film). Patil *et al* reported that the diffusion

coefficient of WO_3 films cycled in H_2SO_4 electrolyte is of the order of 10^{-10} cm^2/s [71]. Hence, the measured diffusion coefficient of WO_3 film is comparable with that reported by other groups [14, 71, 72].

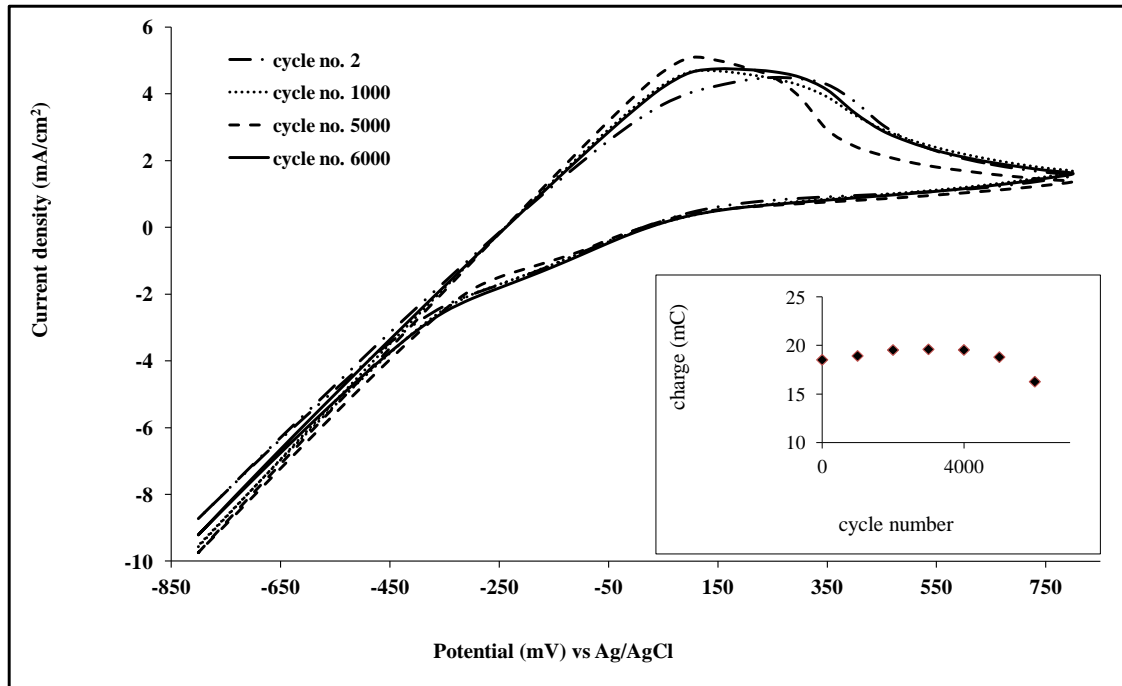


Fig. (4.5): Cyclic Voltammetry of the $\text{W}_{0.95}\text{Ti}_{0.05}\text{O}_3$ film for 2nd, 1000th, 5000th, and 6000th cycles at a scan rate of 200 mV/s. The inset shows stability of the anodic charge with cycle number.

Fig. (4.5) illustrate the stability of $\text{W}_{0.95}\text{Ti}_{0.05}\text{O}_3$ film by measuring its cycle life. The stability of this sample is checked in H_2SO_4 electrolyte by repeating reduction-oxidation cycles between -800 to 800 mV several times at a scan rate of 200mV/s. Fig. (4.5) displays the CV spectra for the film after 2nd and 6000th color- bleach cycles. For the 2nd and 6000th cycles the position of the anodic peak is slightly shifted to lower values, and the current density shifts to higher values. The increase in the current density with cycle's number indicates that the amount of coloring sites available for the redox reaction increases [73]. After 6000th cycles the film degrades and

its material appears in the solution as in Fig. (4.6). The inset in Fig. (4.5) clarifies the stability of the anodic charge with cycle number for $W_{0.95}Ti_{0.05}O_3$ film.



Fig. (4.6): $W_{0.95}Ti_{0.05}O_3$ film degradation after 6000th cycles.

4.1.2 Chronoamperometry (CA)

Chronoamperometry data were recorded for the undoped and Ti doped WO_3 films, with the potential being stepped between -0.5 to +0.5 V vs. Ag/AgCl for 10 s, and appeared in Fig. (4.7).

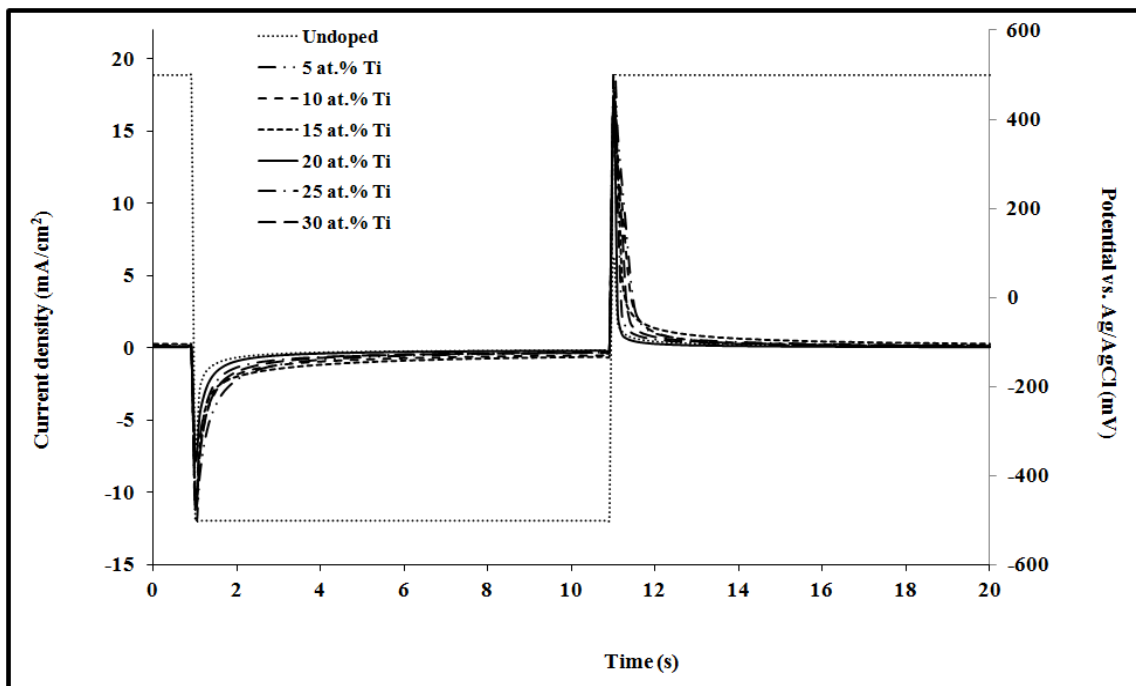


Fig. (4.7): Chronoamperometry of the undoped and 5, 10, 15, 20, 25, and 30 at. % Ti doped WO_3 films at potential step ± 0.5 V for 10 s.

The response time for bleaching (t_b) and coloration (t_c) were measured during Chronoamperometry experiments from Fig. (4.7) and listed in table 4.1 (shown before). All samples show fast switching times, which is comparable with the best results reported by other groups [23]. In general, the coloration operation is slower than the bleaching in WO_3 films, this results is also reported by Ozer *et al* [22].

4.1.3 Optical properties

In addition to electrochemical properties, color change in the visible light is one significant feature of electrochromic devices; the more transmittance in the bleach state (T_b) and less transmittance in color state (T_c) is a requested for efficient electrochromic device. The transmission of light during CA measurements (coloring and bleaching), was done in the three electrode electrochemical cell by the potential switching between -0.5 and +0.5 V vs. Ag/AgCl, in 0.25 M H_2SO_4 solution at $\lambda = 633$ nm.

Fig. (4.8) shows the transmittance change curves for the $W_{0.95}Ti_{0.05}O_3$ electrodes as a function of time. Optical transmittance modulation, of the $W_{0.95}Ti_{0.05}O_3$ film, was measured to be ranges from 61.59 and 73.06 % for coloration and bleaching, respectively. Using the values of transmittance during coloration and bleaching processes, and cathodic charge density value ($Q_c = 9.98$ mC/cm² calculated from Fig. 4.7), the coloration efficiency was calculated using eq. 2.6 and found to be 7.43 cm²/C.

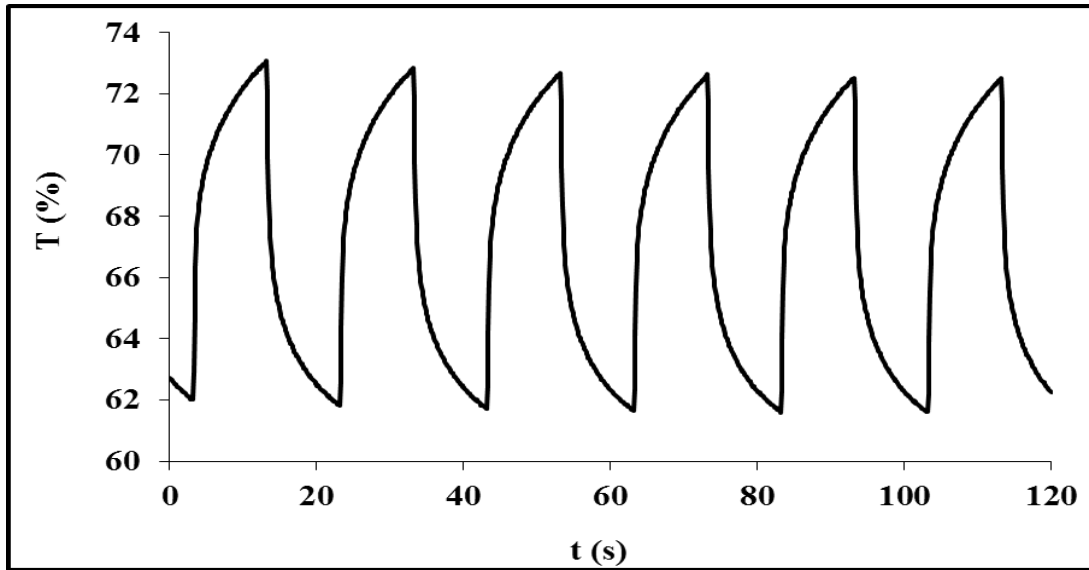


Fig. (4.8): transmittance spectra for $W_{0.95}Ti_{0.05}O_3$ during CA measurements at wavelength of 633nm.

4.1.4 Conclusions

Ti doping effect in electrochromic WO_3 thin films synthesized via dip-coating technique has been investigated. The reversibility, diffusion coefficient, and coloration process of the WO_3 films were improved upon doping with Ti, due to better adherence. The best electrochromic properties were observed for films doped with 5% Ti (which show best CV and reversibility results). The coloration efficiency was calculated for $W_{0.95}Ti_{0.05}O_3$ film and found to be $7.43 \text{ cm}^2/\text{C}$. The stability of $W_{0.95}Ti_{0.05}O_3$ film was checked in H_2SO_4 electrolyte through cycling electrodes up to 6000 reduction/oxidation cycles. Unfortunately, the response time for this film was not the best but still within few seconds range.

4.2 Tungsten oxide co-doped with Ti and Zn (WO_3 : Ti:Zn) thin films

Doping WO_3 with 5 mol. % of Ti results enhanced electrochemical and electrochromic properties in H_2SO_4 electrolyte. However, as quoted before,

co-doped NiO with Ti and Zn greatly enhanced the electrochromic properties by increasing electrochromic coloration efficiency and durability for the films upon cycling [28]. Following same strategy, WO₃ doped with both Ti and Zn electrochromic nano-particles films have been prepared onto FTO/glass substrate for the first time (to our knowledge).

For the films of WO₃ doped with Ti alone, the best sample, in term of electrochromic properties, was found for the WO₃ films that contains molar concentration ratio of 0.05 of Ti (W_{0.95}Ti_{0.05}O₃). Thus, for the WO₃ co-doped with Ti and Zn, the W molar concentration ratio will maintain to 0.95; Zn will compensate Ti species only, as proposed by D. Park [28] for Zn dopant that compensates Ti in the NiO:Ti films. Accordingly, the structure formula can be formed as “W_{0.95}Ti_{0.05-y}Zn_yO₃”.

4.2.1: Cyclic Voltammetry (CV)

Cyclic voltammograms was measured for prepared WO₃ films doped with Ti and Zn (Fig. 4.9). The Zn was prepared with different concentrations that assumed to compensate Ti, as in the structure (W_{0.95}Ti_{0.05-y}Zn_yO₃) with y changes from 0.01 to 0.05 mol. WO₃:Ti:Zn has been done, during 10 cycles in 0.25 M H₂SO₄ electrolyte. The potential was cycled between -800 and 500 mV, against Ag/AgCl reference electrode, at a scan rate of 100 mV/s.

The resulting current densities (J_{pa} and J_{pc}) during bleaching and coloration (oxidation and reduction) have been measured from CV measurements.

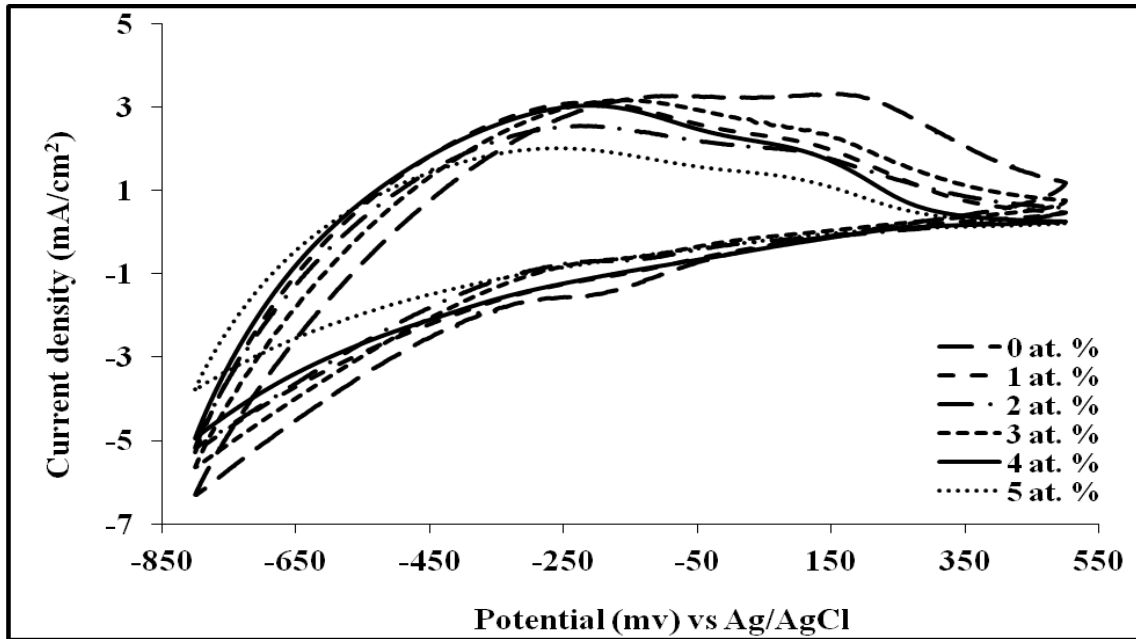


Fig. (4.9): Cyclic voltammetry measurements of the $W_{0.95}Ti_{0.05-y}Zn_yO_3$ with y values 0, 1, 2, 3, 4 and 5 at. % Zn at the scan rate of 100 mV/s.

The dependence of cathodic and anodic peak current density on the Zn doping concentration is displayed in Fig. 4.10 (a) and the corresponding peak potential is appeared in Fig. 4.10 (b).

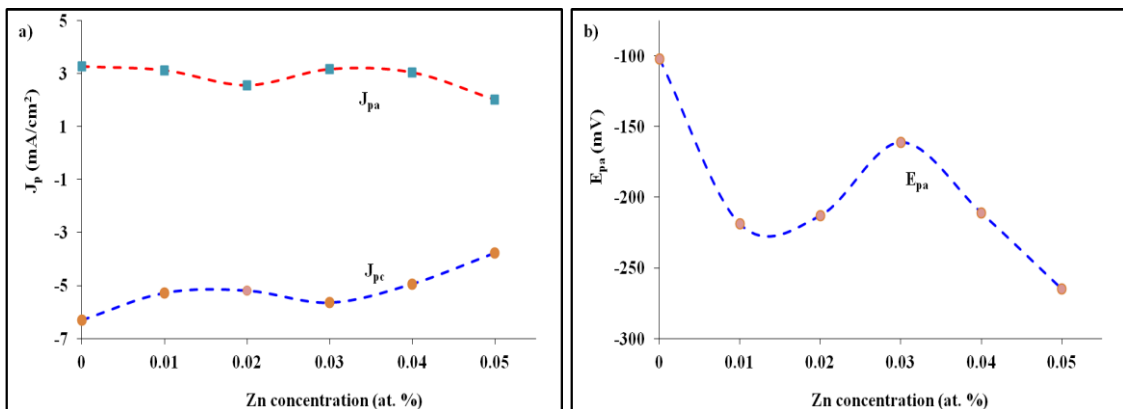


Fig. (4.10): Dependence of (a) peak current density (J_{pa} and J_{pc}), and (b) anodic peak potential (E_{pa}) on Zn concentration.

In the case of Zn doped samples, the cathodic and anodic current densities have comparable values the highest currents are those with 1,3,4 at. % Zn

doped samples. The anodic and cathodic charge densities (Q_a and Q_c respectively) were calculated from current density versus time graph (Fig. 4.11). The ratio of the peak charges (Q_a and Q_c) is calculated for all $WO_3:Ti:Zn$ films and listed in table 4.3.

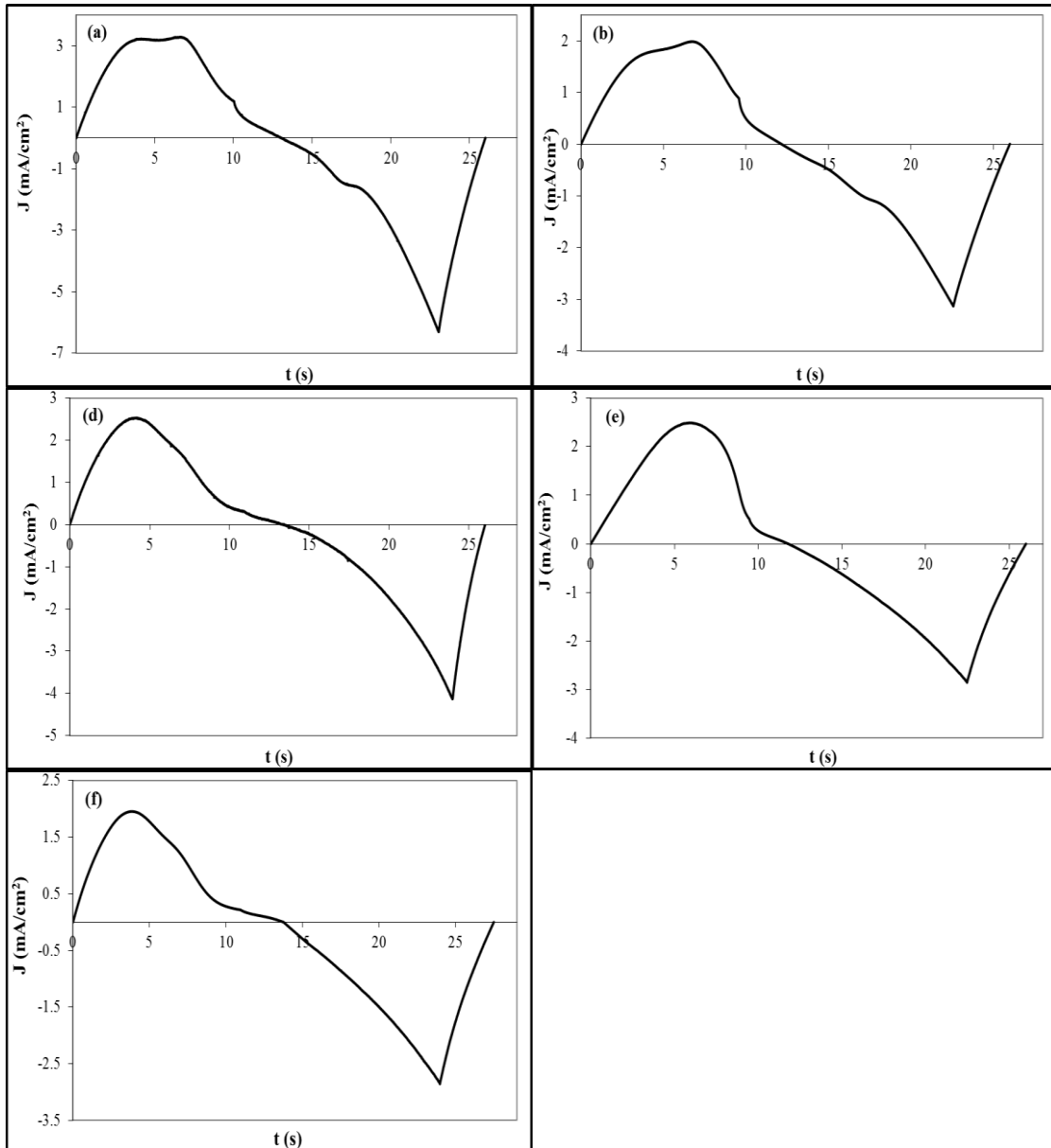


Fig. (4.11): Current density with time for $W_{0.95}Ti_{0.05-y}Zn_yO_3$ ($WO_3:Ti:Zn$) with y values a) 0, b) 0.01, c) 0.02, d) 0.03, e) 0.04, f) 0.05.

As in $\text{WO}_3\text{:Ti}$ films, Q_c is always higher than Q_a , due to quasi reversible reaction. The ratio Q_a/Q_c is generally enhanced for $\text{WO}_3\text{:Ti:Zn}$ films than that of WO_3 doped with Ti alone. This predict that the $\text{WO}_3\text{:Ti:Zn}$ films have enhanced reversibility. The ratio Q_a/Q_c for $\text{WO}_3\text{:Ti:Zn}$ with Zn contents of 3% is found to be the nearest to one. Hence, we can conclude that this film have the best electrochromic properties in term of electrochemical reversibility. This is may be refers to the surface nature of 3% Zn doped $\text{W}_{0.95}\text{Ti}_{0.05}\text{O}_3$ film.

Table (4.3): The electrochromic properties for $\text{W}_{0.95}\text{Ti}_{0.05-y}\text{Zn}_y\text{O}_3$ ($\text{WO}_3\text{:Ti:Zn}$) with y values a) 0, b) 0.01, c) 0.02, d) 0.03, e) 0.04, f) 0.05. Not that the response time presented in the table was deduced from chronoamperometry experiments that will be described later.

Sample Composition	Q_a (mC/cm ²)	Q_c (mC/cm ²)	Q_a/Q_c	Response Time	
				t_c (s)	t_b (s)
$\text{W}_{0.95}\text{Ti}_{0.05}\text{O}_3$	21.59	24.77	0.87	4.4	5.6
$\text{W}_{0.95}\text{Ti}_{0.04}\text{Zn}_{0.01}\text{O}_3$	14.83	17.24	0.86	4.6	2.5
$\text{W}_{0.95}\text{Ti}_{0.03}\text{Zn}_{0.02}\text{O}_3$	14.75	18.26	0.81	4.9	3.2
$\text{W}_{0.95}\text{Ti}_{0.02}\text{Zn}_{0.03}\text{O}_3$	16.69	18.14	0.92	3.9	2.2
$\text{W}_{0.95}\text{Ti}_{0.01}\text{Zn}_{0.04}\text{O}_3$	16.27	18.49	0.88	4.8	3.0
$\text{W}_{0.95}\text{Zn}_{0.05}\text{O}_3$	13.94	16.79	0.83	4.4	2.2

The diffusion coefficient is calculated for $\text{W}_{0.95}\text{Ti}_{0.02}\text{Zn}_{0.03}\text{O}_3$ film using equation 2.3 and the slope of the graph in the inset of Fig. 4.12, it is found to be $9.20\text{E-}10$ cm²/s, which is better than that of $\text{W}_{0.95}\text{Ti}_{0.05}\text{O}_3$ film. Thus, the extent of insertion and extraction of H^+ ions is enhanced for $\text{W}_{0.95}\text{Ti}_{0.02}\text{Zn}_{0.03}\text{O}_3$ film.

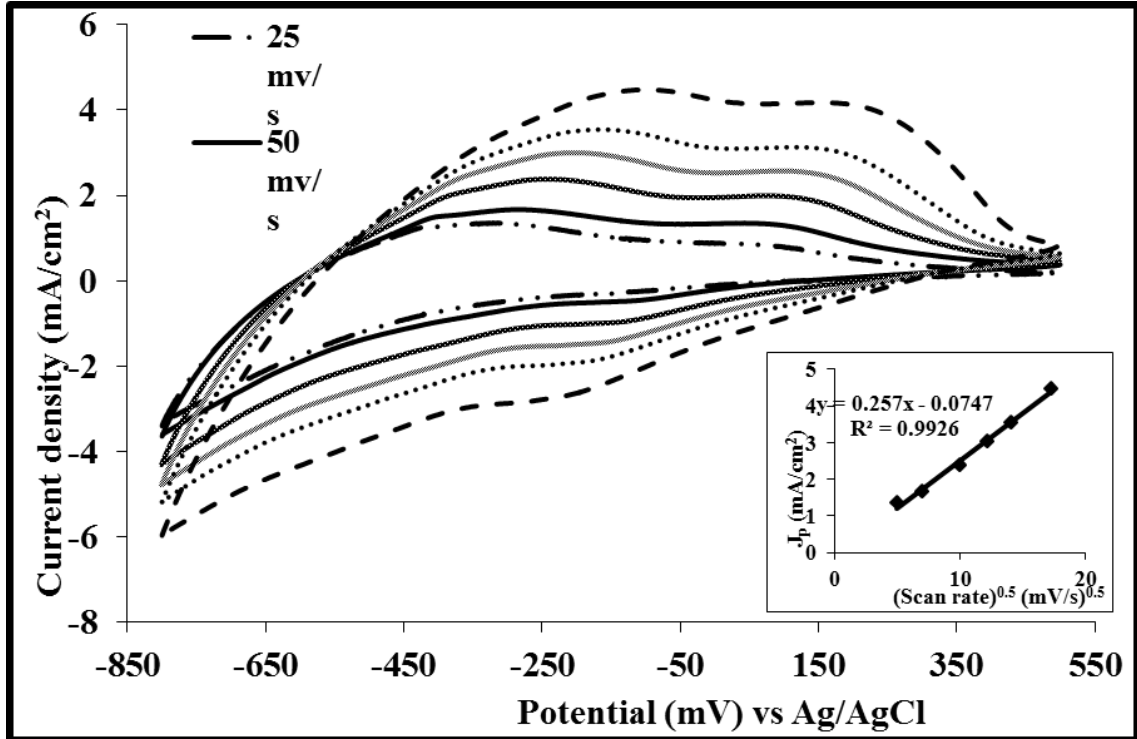


Fig. (4.12): Cyclic voltammetry measurements for $W_{0.95}Ti_{0.02}Zn_{0.03}O_3$ film at different scan rates. The inset shows the reliance of J_{pa} against square root of the scan rate.

The stability of $W_{0.95}Ti_{0.02}Zn_{0.03}O_3$ film is tested in H_2SO_4 electrolyte by repeating color-bleach cycles between -800 to 800 mV several times at a scan rate of 200mV/s. Fig. (4.13) shows the CV spectra for the film for 2nd and 10000th color-bleach cycles. It is appeared that the peak current density increases with cycle's number. In contrast to $W_{0.95}Ti_{0.05}O_3$ film, this increment happens without significant change in the shape or degradation in the film material Fig. (4.13), this predicts that addition of Zn into $W_{0.95}Ti_{0.05}O_3$ film prevents or delays the hydrolysis reaction of Ti dichloride in the mixture. This provides excellent cycling stability of $W_{0.95}Ti_{0.02}Zn_{0.03}O_3$ film. The inset of Fig. (4.13) clarify the stability of the anodic charge with cycle number, which is another indicator of perfect cycling stability of $W_{0.95}Ti_{0.02}Zn_{0.03}O_3$ film.

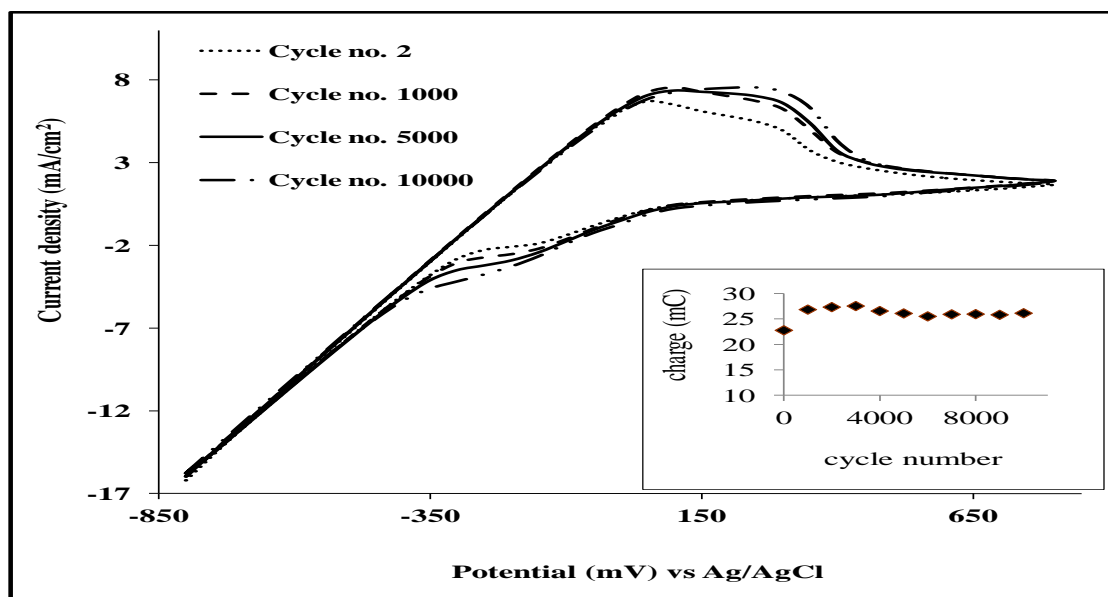


Fig. (4.13): Cyclic Voltammetry of the $W_{0.95}Ti_{0.02}Zn_{0.03}O_3$ film for 2nd, 1000th, 5000th, and 10000th cycles at a scan rate of 200 mV/s. The inset shows stability of the anodic charge with cycle number.

It is observed from Fig. 4.14 that the film material doesn't degrade after 10000th cycles, thus it has longer cycle life than $W_{0.95}Ti_{0.05}O_3$ film.



Fig. (4.14): $W_{0.95}Ti_{0.02}Zn_{0.03}O_3$ film after 10000th cycles.

4.2.2 Chronoamperometry (CA)

Chronoamperometry data were recorded for the undoped and Zn doped $W_{0.95}Ti_{0.05}O_3$ film, with the potential being switched between -0.5 to +0.5 V vs. Ag/AgCl for 10 s, and illustrated in Fig. (4.15).

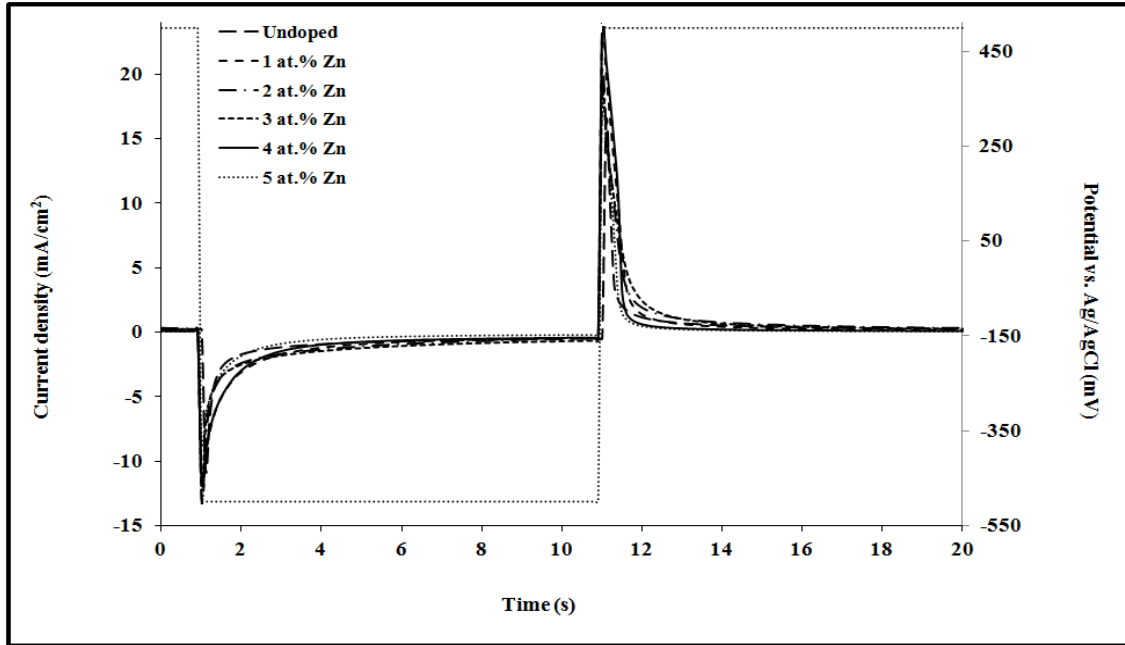


Fig. (4.15): Chronoamperometry of the undoped and 1, 2, 3, 4, and 5 at. % Zn doped $W_{0.95}Ti_{0.05}O_3$ films at potential step ± 0.5 V for 10 s.

The response time for bleaching (t_b) and coloration (t_c) were measured through Chronoamperometry experiments from Fig. (4.15) and listed in table 4.3 (shown before). It offers quick switching times, which is faster than $W_{0.95}Ti_{0.05}O_3$ film in the bleaching process. Between all co-doped samples, $W_{0.95}Ti_{0.02}Zn_{0.03}O_3$ film has the fastest response time during both coloration and bleaching process. The coloration process is noticed to be slower than the bleaching operation in all $WO_3:Ti:Zn$ films.

4.2.3 Optical properties

As quoted before, Color change in the visible light is one significant feature of electrochromic devices; the more increase in the transmission contrast ratio between coloration and bleaching (T_b/T_c) of the electrochromic film, the more efficient the electrochromic apparatus.

Through experimental work, films with Zn contents are observed to have darker blue color during coloration and become more transparent during bleaching process (especially film with 3 at. % Zn). Which predicts that $\text{WO}_3\text{:Ti:Zn}$ films are more efficient as an electrochromic device.

To prove this observation, the transmittance during CA measurements for the $\text{W}_{0.95}\text{Ti}_{0.02}\text{Zn}_{0.03}\text{O}_3$ electrodes was done in the three electrode electrochemical cell. The potential switches between -0.5 and +0.5 V vs. Ag/AgCl, in 0.25 M H_2SO_4 solution at $\lambda = 633$ nm, and plotted in Fig. (4.16). Since the cathodic current is the current for a complete change between coloration and transparency, we can use it to calculate the charge (Q_c) needed to color the layer. Optical transmittance modulation, of the $\text{W}_{0.95}\text{Ti}_{0.02}\text{Zn}_{0.03}\text{O}_3$ film, was measured to be ranges from 38.79 and 89.13 % for coloration and bleaching, respectively. Using the values of transmittance during coloration and bleaching processes, and cathodic charge density value ($Q_c = 17.42$ mC/cm² calculated from Fig. 4.15), the coloration efficiency was calculated using eq. 2.6 and found to be 20.74 cm²/C. Hence, it results in an improved efficiency compared to that of $\text{W}_{0.95}\text{Ti}_{0.05}\text{O}_3$ film. Higher coloration and consequently higher coloration efficiency for $\text{W}_{0.95}\text{Ti}_{0.02}\text{Zn}_{0.03}\text{O}_3$ film means larger surface area are exposed to electrochemical reaction which may be refers to less grain size [41] than that of $\text{W}_{0.95}\text{Ti}_{0.05}\text{O}_3$ film.

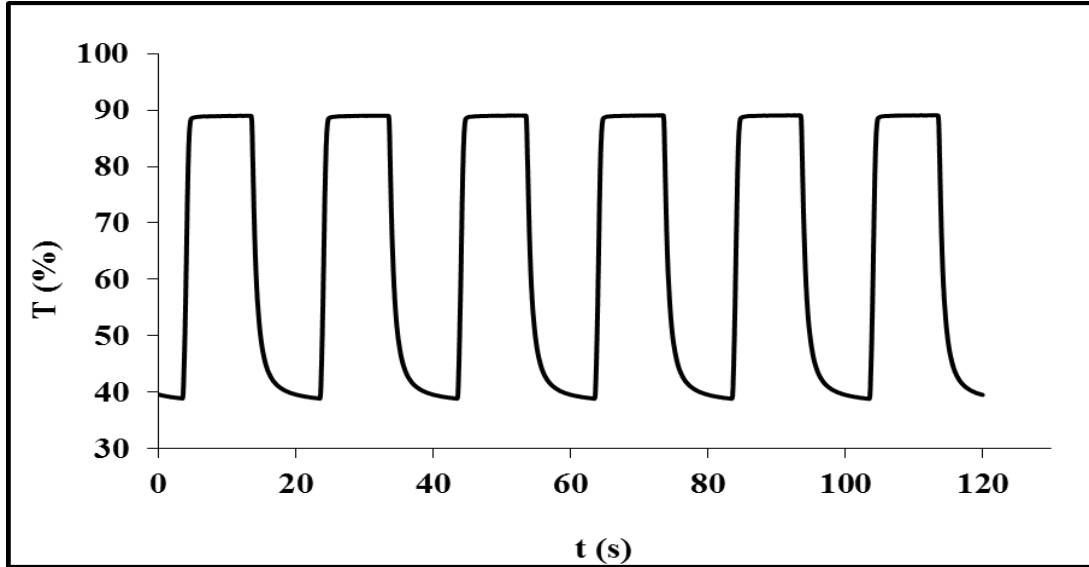


Fig. (4.16): transmittance spectra for $W_{0.95}Ti_{0.02}Zn_{0.03}O_3$ during CA measurements at wavelength of 633nm.

4.2.4 Conclusions

Doping $WO_3:Ti$ with Zn was found to improve the electrochromic properties of the prepared electrochromic films. The reversibility, and coloration process of the $WO_3:Ti$ films are improved upon doping with Zn, due to better adherence. The best electrochromic properties were observed for films doped with 3% Zn (which show best CV and reversibility results). The coloration efficiency was calculated for $W_{0.95}Ti_{0.02}Zn_{0.03}O_3$ film and found to be $20.74 \text{ cm}^2/C$, which is a dramatically enhanced efficiency compared to that of $W_{0.95}Ti_{0.05}O_3$ film. $W_{0.95}Ti_{0.02}Zn_{0.03}O_3$ film was found to be stable in H_2SO_4 electrolyte up to 10000 reduction/oxidation cycles.

4.3 General Conclusions

To have a closer look at our results, let us summarise what we have measured for the three compositions (WO_3 , $W_{0.95}Ti_{0.05}O_3$, and $W_{0.95}Ti_{0.02}Zn_{0.03}O_3$):

- The reversibility was **80 %** for WO_3 , **87%** for $\text{W}_{0.95}\text{Ti}_{0.05}\text{O}_3$, and **92%** for $\text{W}_{0.95}\text{Ti}_{0.02}\text{Zn}_{0.03}\text{O}_3$ film.
- The diffusion coefficient was **4.80E-11** cm^2/s for WO_3 , **4.87E-10** cm^2/s for $\text{W}_{0.95}\text{Ti}_{0.05}\text{O}_3$, and **9.2E-10** cm^2/C for $\text{W}_{0.95}\text{Ti}_{0.02}\text{Zn}_{0.03}\text{O}_3$ film.
- The stability is checked up to **6000th** reduction/oxidation cycles for $\text{W}_{0.95}\text{Ti}_{0.05}\text{O}_3$, while $\text{W}_{0.95}\text{Ti}_{0.02}\text{Zn}_{0.03}\text{O}_3$ stability is tested up to **10000** reduction/ oxidation cycles.
- Bleaching and coloration times (t_b, t_c) was measured to be **(3,5.3)** for WO_3 , **(5.6,4.4)** for $\text{W}_{0.95}\text{Ti}_{0.05}\text{O}_3$, and **(2.2,3.9)** for $\text{W}_{0.95}\text{Ti}_{0.02}\text{Zn}_{0.03}\text{O}_3$ film, respectively.
- The coloration efficiency was **7.43** cm^2/C for $\text{W}_{0.95}\text{Ti}_{0.05}\text{O}_3$ and **20.74** cm^2/C for $\text{W}_{0.95}\text{Ti}_{0.02}\text{Zn}_{0.03}\text{O}_3$ film.

From the above results, it's clear that doping WO_3 with 5% of Ti ($\text{W}_{0.95}\text{Ti}_{0.05}\text{O}_3$) enhance the electrochemical and the electrochromic properties over that of the undoped WO_3 films. On the other hand, co-doping WO_3 with nominal concentration of Ti and Zn ($\text{W}_{0.95}\text{Ti}_{0.02}\text{Zn}_{0.03}\text{O}_3$) greatly improves the electrochemical and the electrochromic properties over that of the Ti single doped WO_3 .

Suggestions for Further Works

The author suggest the following for the new electrochromic electrode $\text{WO}_3:\text{Ti}:\text{Zn}$ for future work:

1. Doing more analysis for the films as: XRD, PL, SEM, TEM, AFM, etc.

2. Preparing WO_3 thin films using different techniques such as: Electrochemical Deposition (ECD), Chemical Bath Deposition (CBD).
3. Studying the electrochromic properties when the films annealing with different temperatures.
4. Studying the effect of thickness on electrochromic properties.
5. Studying the previous films characteristics with different electrolytes and different electrolyte concentrations.
6. Doping with different materials such as: Sn, F, Li, etc.

References

- [1] G. Eranna, *Metal Oxide Nanostructures as Gas Sensing Devices*, CRC Press, united states of America, (2011) P.134.
- [2] Aline Rougier, *Electrochromic Materials and Applications: Proceedings of the International Symposium Volumes 2003-2017 of Proceedings (Electrochemical Society)*, The Electrochemical Society, Pennington, (2003) P. 41, P. 104.
- [3] K. V. Madhuri, P. V. Ashrit, *Effect of substrate on the electrochromic properties of Tungsten oxidethin films*, **International Journal of Engineering & Technology**, **3** (2) (2014) 245-251.
- [4] C. G. Granquist, *Electrochromic oxides: A unified view*, **Solid State Ionics**, **70-71** (1) (1994) 678-685.
- [5] Mino Green, W.C. Smith, J.A. Weiner, *A thin film electrochromic display based on the tungsten bronzes*, **Thin Solid Films**, **38** (1) (1976) 89-100.
- [6] T. He and J. Yao, *Photochromic materials based on Tungsten oxide*, **Journal of Materials Chemistry**, **17** (43) (2007) 4547–4557.
- [7] S. K. Deb, *Optical and Photoelectric Properties and Colour Centres in Thin Films of Tungsten oxide*, **Philosophical Magazine**, **27** (4) (1973) 801-822.
- [8] Erik Lassner, Wolf-Dieter Schubert, *Tungsten: Properties, Chemistry, Technology of the Elements, Alloys, and Chemical Compounds*, Springer, New York, (1999) P.260.
- [9] Noboru Oyama, Viola Birss, Electrochemical Society. Physical Electrochemistry Division, Electrochemical Society. Meeting,

Proceedings of the Symposium on Molecular Functions of Electroactive Thin Films, The Electrochemical Society, Pennington, (1999) P.152.

- [10] R.sivakumar, A. Moses Ezhil Raj, B. Subramanian, M. jayachandran, D.C. Trivedi, C. Sanjeeviraja, *Preparation and characterization of spray deposited n-type WO₃ thin films for electrochromic devices*, **Materials Research Bulletin**, **39** (10) (2004) 1479-1489.
- [13] Shiyarovskaya, M. Hepel, E. Tewksbury, *Electrochromism in electrodeposited nanocrystalline WO₃ films I. Electrochemical and optical properties*, **New Materials for Electrochemical Systems**, **3** (3) (2000) 241-247.
- [15] An-Hui Lu, Dongyuan Zhao, Ying Wan, *Nanocasting: A Versatile Strategy for Creating Nanostructured Porous Materials*, Royal Society of Chemistry, New York, (2010) P.49.
- [14] K. Punitha, R. Sivakumar, C. Sanjeeviraja, *Enhanced Colouration Efficiency of Pulsed DC Magnetron Sputtered WO₃ Films Cycled in H₂SO₄ Electrolyte Solution*, **Smart Materials Research**, **2014** (2014) 9.
- [15] An-Hui Lu, Dongyuan Zhao, Ying Wan, *Nanocasting: A Versatile Strategy for Creating Nanostructured Porous Materials*, Royal Society of Chemistry, New York, (2010) P.49.
- [16] Simona Badilescu, P.V. Ashrit, *Study of sol-gel prepared nanostructured WO₃ thin films and composites for electrochromic applications*, **Solid State Ionics**, **158** (1-2) (2003) 187-197.

- [17] C. Cantalini, M. Z. Atashbar, Y. Li, M. K. Ghantasala, S. Santucci, W. Wlodarski, M. Passacantando, *Characterization of sol-gel prepared WO_3 thin films as a gas sensor*, **Journal of Vacuum Science & Technology A**, **17** (4) (1999) 1873.
- [18] Hyo-Jin Ahn, Hee-Sang Shim, Yung-Eun Sung, Tae-Yeon Seong, Won Bae Kim, *Electrochromism of Sn-Modified WO_3 Electrodes Prepared from Sol-Gel Method*, **Electrochemical and Solid-State Letters**, **10** (12) (2007) E27-E30.
- [19] Chen, Ya-Chi; Lin, Tai-Nan; Chen, Tien-Lai; Li, Yun-Da; Weng, Ko-Wei, *Electrochromic properties of tungsten-titanium oxide films*, **Journal of Nanoscience and Nanotechnology**, **12** (2) (2012) 1296-1300.
- [20] S. Reich, Y. Tsabba, *Possible nucleation of a 2D superconducting phase on WO single crystals surface doped with Na*, **The European Physical Journal B**, **9** (1) (1999) 1-4.
- [21] X.F. Cheng, W.H. Leng, D.P. Liu, J.Q. Zhang, C.N. Cao, *Enhanced photoelectrocatalytic performance of Zn-doped WO_3 photocatalysts for nitrite ions degradation under visible light*, **Chemosphere**, **68** (10) (2007) 1976-1984.
- [22] Nilgun Ozer, Nilgun Dogan, *Study of electrochromism in $Ti:WO_3$ films by sol-gel process*, **Inorganic Optical Materials**, **3424** (1998) 106-114.

- [23] Suvarna R. Bathe, P.S. Patil, *Titanium doping effects in electrochromic pulsed spray pyrolysed WO₃ thin films*, **Solid State Ionics**, **179** (9-10) (2008) 314-323.
- [24] C. V. Ramana, Gaurav Baghmar, Ernesto J. Rubio, and Manuel J. Hernandez, *Optical constants of amorphous, transparent titanium-doped Tungsten oxide thin films*, **ACS Appl. Mater Interfaces**, **5** (11) (2013) 4659- 4666.
- [25] Zhongchun Wang, Xingfang Hu, *Electrochromic properties of TiO₂-doped WO₃ films spin-coated from Ti-stabilized peroxotungstic acid*, **Electrochimica Acta**, **46** (13-14) (2001) 1951-1956.
- [26] Chenxi Yang, Jian-Feng Chen, Xiaofei Zeng, Daojian Cheng, and Dapeng Cao, *Design of the Alkali-Metal-Doped WO₃ as a Near-Infrared Shielding Material for Smart Window*, **American Chemical Society**, **53** (46) (2014) 17981-17988.
- [27] R Long, NJ English, *First-principles calculation of nitrogen-tungsten codoping effects on the band structure of anatase-titania*, **Applied Physics Letters**, **94** (13) (2009) 132102 - 132102-3.
- [28] Dae Hoon Park, *Optimization of nickel oxide- based electrochromic thin films*, Ph. D. Thesis, Bordeaux I University, France, (2006).
- [29] Evans, Rachel C., Douglas, Peter, Burrow, Hugh D., *Applied Photochemistry, 1st Ed*, Springer Netherlands, Dublin, (2013) P. 176.
- [30] Linert, Wolfgang, *Highlights in Solute-Solvent Interactions, 1st Ed*, Springer-Verlag Wien, Vienna, (2002) P. 43.

- [31] Heinz Dürr, Henri Bouas-Laurent, *Photochromism: Molecules and Systems: Molecules and Systems, 1st Ed*, Gulf Professional Publishing, Amsterdam, (2003) P. 30, P. 33.
- [32] Kanji Kajiwara, *Gels Handbook, Four-Volume Set*, Academic Press, United State of America, (2000) P. 226.
- [33] Peter Bamfield, Michael G. Hutchings, *Chromic Phenomena: Technological Applications of Colour chemistry, 2nd Ed*, Royal Society of Chemistry, New York, (2010) P. 59, 86.
- [34] Jin Min Wang, Xiao Wei Sun, and Zhihui Jiao, *Application of Nanostructures in Electrochromic Materials and Devices: Recent Progress, Materials*, **3** (12) (2010) 5029-5053.
- [35] C.G. Granqvist, *Handbook of Inorganic Electrochromic Materials*, Elsevier, Amsterdam, (1995) P.1.
- [36] Claes G. Granqvist, *Transparent conductors as solar energy materials: A panoramic review, Solar Energy Materials and Solar Cells*, **91** (17) (2007) 1529-1598.
- [37] Gregory J. Exarhos, Xiao-Dong Zhou, *Discovery-based design of transparent conducting oxide films, Thin Solid Films*, **515** (18) (2007) 7025-7052.
- [38] I. Saadeddin, *Preperation and characterization of new transparent conducting oxides based on SnO₂ and In₂O₃;ceramics and thin films*, Ph. D. thesis, Bordeaux I University, Bordeaux, France, 2007.
- [39] Bruno Scrosati, *Applications of Electroactive Polymers, 1st Ed*, Springer Science & Business Media, London, (1993) P. 250.

- [40] Agnieszka, Pawlicka, *Development of Electrochromic Devices*, **Bentham Science Publishers**, **3** (3) (2009) 177-181(5).
- [41] Atheer Yousef Saleh Abu-Yaqoub, *Electrochromic Properties of Sol-gel NiO – based films*, Master Theses, An-Najah National University, Nablus, Palestine, 2012.
- [42] Søren Prip Beier, Peter Dybdahl Hede, *Essentials of Chemistry*, **2nd Ed**, Bookboon, London, (2010) P.82.
- [43] National Research Council (U.S.). Committee on Technical Aspects of Critical and Strategic Material. Panel on Trends in Usage of Tungsten, *Trends in Usage of Tungsten: Report*, National Academies, Washington, (1973) P.77.
- [44] Laura Mendicino, Electrochemical Society. Dielectric Science and Technology Division, *Environmental Issues with Materials and Processes for the Electronics and Semiconductor Industries: Proceedings of the Fourth International Symposium*, the Electrochemical Society, Pennington, (2001) P.180.
- [45] Wei Hao Lai, Yen Hsun Su, Lay Gaik Teoh, Yuan Tsung Tsai and Min Hsiung Hon, *Synthesis of Tungsten oxide Particles by Chemical Deposition Method*, **Materials Transactions**, **48** (6) (2007) 1575-1577.
- [46] Sibuyi, Praise, *Nano-rods WO₃- δ for electrochromic smart windows applications*, **Magister Scientiae**, University of Western Cape, Cape Town, South Africa, 2006.

- [47] Agus Purwanto, Hendri Widiyandari, Takashi Ogi, Kikuo Okuyama, *Role of particle size for platinum-loaded Tungsten oxide nanoparticles during dye photodegradation under solar-simulated irradiation*, *Catalysis Communications*, **12** (6) (2011) 525–529.
- [48] Juan M. Coronado, Fernando Fresno, María D. Hernández-Alonso, Raquel Portela, *Design of Advanced Photocatalytic Materials for Energy and Environmental Applications*, Springer Science & Business Media, Nova Gorica, (2013) P.108.
- [49] S.K. Deb, *A Novel Electrophotographic System*, *Applied Optics*, **8** (101) (1969) 192-195.
- [50] I. Shiyonovskaya and M. Hepel, *Isotopic Effects in Cation Injected Electrochromic Films*, *J. Electrochem. Soc.*, **145** (3) (1998) 1023-1028.
- [51] B. Vuillemin and O. Bohnke, *Kinetics study and modelling of the electrochromic phenomenon in amorphous Tungsten oxidethin films in acid and lithium electrolytes*, *Solid State Ionics*, **68** (3-4) (1994) 257-267.
- [52] A. Nakamura, S. Yamada, *Fundamental absorption edge of evaporated amorphous WO_3 films*, *J. Appl. Phys.*, **24** (1) (1981) 55-59.
- [53] S. Hashimoto and H. Matsuoka, *Mechanism of electrochromism for amorphous WO_3 thin films*, *J. Appl. Phys.*, **69** (2) (1991) 933.

- [54] Joseph Wang, *Electroanalytical Techniques in Clinical Chemistry and Laboratory Medicine*, John Wiley & Sons, Las cruces, (1988) P.20.
- [55] H. K. MOUDGIL, *TEXTBOOK OF PHYSICAL CHEMISTRY*, 2nd Ed, PHI Learning Pvt. Ltd., Delhi, (2014) P.376, P.576.
- [56] Rosemary A. Marusak, Kate Doan, Scott D. Cummings, *Integrated Approach to Coordination Chemistry: An Inorganic Laboratory Guide*, John Wiley & Sons, Hoboken, (2007) P.95.
- [57] Allen J. Bard, György Inzelt, Fritz Scholz, *Electrochemical Dictionary*, 2nd Ed, Springer Science & Business Media, Austin, (2012) P.129.
- [58] D. Calloway, *Beer –Lambert law*, **Journal of Chemical Education**, **74** (7) (1997) 744.
- [59] Faiz Mohammad, *Specialty Polymers: Materials and Applications*, I. K. International Pvt Ltd, New Delhi, (2007) P.61.
- [60] Paul Monk, Roger Mortimer, David Rosseinsky, *Electrochromism and Electrochromic Devices*, Cambridge University Press, New York, (2007) P.10.
- [61] Arthur A. Tracton, *Coatings Technology: Fundamentals, Testing, and Processing Techniques*, 3rd Ed, CRC Press, United State of America, (2006) P.31.1.
- [62] Kouros Kalantar-zadeh, Benjamin Fry, *Nanotechnology-Enabled Sensors*, Springer Science & Business Media, Melbourne, (2007) P.153.

- [63] Hans H. Gatzert, Volker Saile, Jürg Leuthold, *Micro and Nano Fabrication: Tools and Processes*, Springer, Garbsen, (2015) P.93.
- [64] Sahar Mustafa Asad Khudruj, *CdS Thin Film Photo-Electrochemical Electrodes: Combined Electrochemical and Chemical Bath Depositions*, Magister Theses, An-Najah National University, Nablus, Palestine, 2011.
- [65] Theodor Schneller, Rainer Waser, Marija Kosec, David Payne, *Chemical Solution Deposition of Functional Oxide Thin Films*, Springer Science & Business Media, Aachen, (2014) P. 143.
- [66] Noorhana Yahya, *Carbon and Oxide Nanostructures: Synthesis, Characterisation and Applications*, Springer Science & Business Media, Malaysia, (2011) P.358.
- [67] Sam Zhang, *Nanostructured Thin Films and Coatings: Functional Properties*, CRC Press, Boca Rotan, (2010) P. 218, P. 13.
- [68] Ghenadii Korotcenkov, *Handbook of Gas Sensor Materials: Properties, Advantages and Shortcomings for Applications Volume 2: New Trends and Technologies*, Springer Science & Business Media, Gwangju, (2013) P.28.
- [69] Mailadil T. Sebastian, *Dielectric Materials for Wireless Communication*, Elsevier, Amsterdam, (2010) P.77.
- [70] Karla R. Reyes-Gil, Zachary D. Stephens, Vitalie Stavila, and David B. Robinson, *Composite WO_3/TiO_2 nanostructures for high electrochromic activity*, *ACS Appl. Mater. Interfaces*, 7 (4) (2015) 2202–2213.

- [71] P. S. Patil, P. R. Patil, S. S. Kamble, and S. H. Pawar, *Thickness-dependent electrochromic properties of solution thermolyzed Tungsten oxide thin films*, **Solar Energy Materials and Solar Cells**, **60** (2) (2000) 143–153.
- [72] E. Cazzanelli, C. Vinegoni, G. Mariotto, A. Kuzmin, J. Purans, *Raman study of the phase transitions sequence in pure WO_3 at high temperature and in H_xWO_3 with variable hydrogen content*, **Sol. State Ionics**, **123** (1-4) (1999) 67-74.
- [73] A. Al-Kahlout, S. Heusing, M.A. Aegerter, *Electrochromism of $NiOTiO_2$ sol-gel layer*, **Journal of Sol-Gel Science and Technology**, **39** (2) (2006) 195-206.

جامعة النجاح الوطنية
كلية الدراسات العليا

الخصائص الكهروكيميائية لطبقات السائل الهلامي لاكسيد الثنجستن المطعمة بالتيتانيوم والزنك

إعداد

مدلين أحمد محمد البلشه

إشراف

د. إياد سعد الدين

د. محمد سليمان

قدمت هذه الأطروحة استكمالاً لمتطلبات الحصول على درجة الماجستير في الفيزياء بكلية الدراسات العليا في جامعة النجاح الوطنية في نابلس - فلسطين.

2016

ب

الخصائص الكهروكيميائية لطبقات السائل الهلامي لأكسيد التنجستن المطعمة بالتيتانيوم

والزنك

إعداد

مدلين أحمد محمد البلشه

إشراف

د. إياد سعد الدين

د. محمد سليمان

المخلص

في هذا البحث تم تحضير أفلام WO_3 الرقيقة النانوية على شرائح من الزجاج الموصل (FTO/glass) باستخدام طريقة السول-جل (الطلاء بالغمس). طعمت هذه الأفلام بمركبات عنصري التيتانيوم (Ti) والزنك (Zn) بتركيز مختلفة 5-30% للعنصر الأول ومن 1-5% للعنصر الثاني. تم دراسة خصائص عدة لتلك الشرائح بهدف المقارنة بينها، منها: سلوكها الكهروكيميائي واقتران الفولتية الدوري و أطياف النفاذية. تم دراسة الية التلوين أثناء التجارب المختلفة في المحلول الكهربي 0.25 مولار من حمض الكبريتيك، وحسبت كذلك كمية الشحنة الداخلة والخارجة من الطبقة خلال عملية التلوين بالإضافة الى فعالية التلوين. تم فحص استقرار العينات في حمض الكبريتيك ل 6000 دورة على الأقل. كل النتائج أشارت الى أن تطعيم مادة أكسيد التنجستون بالتيتانيوم والزنك معا بتركيز محددة يحسن من التلوين الكهربائي لأكسيد التنجستون مقارنة بتلك المطعمة بالتيتانيوم لوحده.